Title: Strigolactone effects on *Sorghum bicolor* ecophysiology and symbioses

Authors: Chloee M. McLaughlin[1,2*], Margarita Takou[2,3], Joel Masanga[2], Erica H. Lawrence-Paul[2], Evelyn J. Abraham[1, 4], Melanie Perryman[5], Anna Calabritto[6], Amandeep Cheema[7], Baloua Nebie[8], Steven Runo[9], Joshua J. Kellogg[1],[10], Roberta Croce[6], Daniel P. Schachtman[11], Huirong Gao[12], Ruairidh J. H. Sawers[5], Jesse R. Lasky[2, 13]

[1] Intercollege Graduate Degree Program in Plant Biology, Pennsylvania State University, University Park, PA, U.S.A.
[2] Department of Biology, Pennsylvania State University, University Park, PA, U.S.A.
[3] Institute for Plant Sciences, University of Cologne, Cologne, Germany
[4] Centera Bioscience Inc., Tempe, AZ, U.S.A.
[5] Department of Plant Science, Pennsylvania State University, University Park, PA, U.S.A.
[6] Department of Physics and Astronomy and Institute for Lasers, Life and Biophotonics, Faculty of Sciences, VU University Amsterdam, 1081 HV Amsterdam, Netherlands
[7] Department of Biology and Program in Cell and Molecular Biology, Colorado State University, Fort Collins, CO U.S.A.
[8] West and Central Africa sorghum improvement Program, International Maize and Wheat Improvement Center (CIMMYT), Dakar, Senegal
[9] Department of Biochemistry and Biotechnology, Kenyatta University, Nairobi, Kenya
[10] Department of Veterinary & Biomedical Sciences, Pennsylvania State University, University Park, PA, U.S.A.
[11] Department of Agronomy and Horticulture, and Center for Plant Science Innovation, University of Nebraska-Lincoln, Lincoln, NE, U.S.A.
[12] Corteva Agriscience, Johnston, IA, U.S.A.
[13] PAC Herbarium, Pennsylvania State University, University Park, Pennsylvania, PA, U.S.A.

* Correspondence CMM (cmclaughlin@hudsonalpha.org)

The author responsible for distribution of materials integral to the findings presented in this article in accordance with the policy described in the Instructions for Authors (https://academic.oup.com/plphys/pages/General-Instructions) is Chloee M. McLaughlin.

Running head: Strigolactone effects on *Sorghum bicolor*

Abstract: Strigolactones are ecologically, developmentally, and physiologically important hormones, but much remains unknown about their evolution and role in non-model species. Sorghum is an important C_4 cereal for ~1 billion people globally and exhibits natural variation in root-exuded strigolactones. Differences in sorghum strigolactone stereochemistry are associated with resistance to a parasitic plant, but with evidence for potential trade-offs. In the present study, we studied sorghum mutants of loci in the strigolactone biosynthetic pathway, C*AROTENOID CLEAVAGE DIOXYGENASE 8* (*CCD8*) and *LOW GERMINATION STIMULANT 1* (*LGS1*). We found that *CCD8* CRISPR-Cas9 deletions changed the accumulation of low abundance metabolites, reduced net carbon assimilation rate, altered root architecture and anatomy, and reduced the establishment and benefit of mycorrhizal symbionts. For *LGS1* CRISPR-Cas9 deletions, we found net carbon assimilation rate to be reduced, the colonization of mycorrhizal symbionts to be delayed, and evidence for regulatory pathways involved in stress response and growth to be impacted. We further tested the impacts of restoring functionality of *LGS1* into a normally non-functional background (RTx430). Notably, we did not see consistent impacts of *LGS1* loss-of-function across *LGS1* deletion and insertion mutants, though root exudates from insertion mutants increased stimulation of *Striga* germination, suggesting that background specific modifiers may buffer the strigolactone impacts of loss-of-function at *LGS1*. Our study begins to give context to the trade-offs associated with a host resistance strategy to a parasitic plant and more broadly contributes to understanding the role strigolactones play in sorghum physiological processes, growth, and development.

Introduction

Strigolactones, originally named for their role as germination stimulants to the parasitic plant *Striga* spp. (Cook et al., 1966) are well established as an important class of hormones for plant biology and ecological interactions (Saeed et al., 2017; F. Wu et al., 2022). Strigolactones play key roles in various aspects of plant growth, physiology, and symbiotic interactions, including the regulation of shoot architecture, root development, light harvesting complexes, and associations with mycorrhizal fungi (Akiyama et al., 2005; Gomez-Roldan et al., 2008; Mayzlish-Gati et al., 2010; Ruyter-Spira et al., 2011). Further, as signaling molecules, strigolactones enable plants to regulate their growth and development in response to the external environment (Barbier et al., 2023). To date, more than 30 strigolactones have been characterized which differ in their structure (Yoneyama & Brewer, 2021), though much of the functional variation associated with this structural diversity remains to be elucidated.

Strigolactones are synthesized from carotenoids which undergo catalytic reactions by several enzymes. Their biosynthesis begins with the isomerization of β-carotene from a trans to a cis configuration by β-carotene isomerase (*DWARF27*, *D27*). 9-cis-β-carotene is then cleaved by two carotenoid cleavage dioxygenases, *CAROTENOID CLEAVAGE DIOXYGENASE 7* (*CCD7*) and *CAROTENOID CLEAVAGE DIOXYGENASE 8* (*CCD8*), resulting in the formation of carlactone (Alder et al., 2012; Seto et al., 2014). Mutants of *CCD7* and *CCD8* have undetectable or extremely reduced exudation of strigolactones (tomato, *SlCCD8 (Kohlen et al., 2012)*; sorghum, *SbCCD8* (Hao et al., 2023); rice, *OsCCD7* (Butt et al., 2018)) confirming the importance of carotenoid cleavage dioxygenases in strigolactone biosynthesis.

Studies have found that mutants in homologs of *CCD7* and *CCD8* are strigolactone deficient and have altered shoot tillering and branching in multiple plant species including

Arabidopsis, rice, tomato, tobacco, maize, and sorghum (Arite et al., 2012; Gao et al., 2018; Hao et al., 2023; Sorefan et al., 2003; Vogel et al., 2010). Additionally, the role of strigolactones in modulating root system morphology has been documented in multiple plant species, increasing the length of primary roots in tomato, root hairs in *Arabidopsis*, suppressing the formation of adventitious roots in pea, and enhancing crown root growth in rice (Arite et al., 2012; Kohlen et al., 2012; Rasmussen et al., 2012; Urquhart et al., 2015). It should be noted that strigolactone regulation of root development is dependent on the plant species and growth conditions. Moreover, in *Arabidopsis* strigolactone signaling mutants differentially accumulated root metabolites and had a notable reduction in flavonols (Walton et al., 2016) which are involved in root development (Maloney et al., 2014). More recently, (Zhao et al., 2025) identified that strigolactone signaling negatively influenced cambium-derived xylem element vessel formation in *Arabidopsis*, further supporting that strigolactones impact root development and variation related to water use and stress response. Beyond playing a role in plant architecture and anatomy, strigolactones have been implicated as participating in plant response to light and modulating photosynthesis potentially by influencing stomatal behavior (Van Ha et al., 2014), chlorophyll content and the efficiency of light capture through transcriptional regulation (Mayzlish-Gati et al., 2010). Transcriptome analysis of strigolactone deficient tomato mutants (*Sl-ORT1*) revealed decreased expression of genes involved in light harvesting. Treatment with the synthetic strigolactone analog GR24 led to increased expression of these genes (Mayzlish-Gati et al., 2010; Van Ha et al., 2014), which suggests that strigolactones are positive regulators of light harvesting processes. Altogether, the number of phenotypes regulated by or associated with strigolactones points to their critical role in plant responses to the environment and their downstream impacts on numerous complex traits.

Along with other plant hormones, strigolactones play a key role in signaling pathways that integrate nutrient and environmental cues to form beneficial symbioses. For example, plants have evolved the phosphate starvation response (PSR) which reprograms plant processes to acquire more phosphorus from the environment and to remobilize phosphorus under nutrient-deprived conditions (Chien et al., 2018; Zhang et al., 2014). The plant PSR results in an increase of synthesis and exudation of strigolactones (Haider et al., 2023; Y. Wang et al., 2021). This increase in strigolactone provides two crucial functions: first to serve as endogenous hormones that control plant development and stress response, and secondly, to serve as exogenous signaling molecules and promote symbiosis with beneficial arbuscular mycorrhizal fungi (AMF). AMF are obligate heterotrophs that interact with the roots of more than 80 percent of land plants, including crop plants, and provide difficult to access nutrients in return for photosynthetically fixed carbon and lipids (Brundrett & Tedersoo, 2018). The fungi colonize the host root cortex before differentiating into highly branched structures called arbuscules, the main site of nutrient exchange between the fungal and plant symbiotic partners. Strigolactones play a key role in the initiation of the symbiosis by inducing AMF hyphal branching, enhancing the possibility of contact between AMF and a host root (Giovannetti et al., 1993, 1994; Kodama et al., 2022).

Host exudation of strigolactones as a signal to recruit AMF symbionts has been hijacked by parasitic plant members of the Orobanchaceae family. Obligate root parasites in this family germinate after sensing host root exuded strigolactones (Yoneyama et al., 2010). Of particular interest is the obligate root parasite *Striga hermonthica,* which accounts for billions of dollars' worth of annual cereal crop damage in tropical Africa and is considered one of the greatest constraints to African food security (Spallek et al., 2013). One of the best characterized host

resistance mechanisms is low germination of *Striga* by the host's root exudates (Gurney et al., 2003; Mallu et al., 2021; Ruyter-Spira et al., 2011). In sorghum, naturally occurring deletion mutants of the *LOW GERMINATION STIMULANT 1* (*LGS1*) gene confer shifts in strigolactone stereochemistry, where orobanchol rather than 5-deoxystrigol becomes the more abundant strigolactone in root exudates (Gobena et al., 2017). The gene responsible for the low germination stimulation phenotype encodes a sulfotransferase, which functions downstream of CYP711A (SbMAX1a), converting 18-hydroxy-carlactonoic acid (18-hydroxy-CLA) into 5-deoxystrigol and 4-deoxyorobanchol simultaneously (S. Wu & Li, 2021; Yoda et al., 2021). Beyond alterations in the specific strigolactones exuded, there is evidence that loss of function *lgs1* mutants are characterized by overall low strigolactone exudation (Bellis et al., 2020).

Though loss-of-function at *LGS1* might increase sorghum's fitness in landscapes with parasite pressure, changes to strigolactone biosynthesis may be detrimental to endogenous processes in sorghum. Relatedly, Bellis et al., (2020) found evidence of potential trade-offs of *LGS1* loss-of-function: natural loss-of-function *lgs1* alleles are maintained at a modest frequency in sorghum landraces even within *S. hermonthica*-prone regions (up to ~30% in northern Nigeria) and are nearly absent in *S. hermonthica*-free landscapes. CRISPR-Cas9 deletions of LGS1 had altered expression of >2,000 genes compared to the wild type, especially the downregulation of light harvesting genes in shoots (Bellis et al., 2020). Given the broad roles strigolactones play in plant processes and previous evidence for trade-offs associated with maintaining *lgs1*, we hypothesized that sorghum with loss-of-function at *LGS1* will be subject to trade-offs through pleiotropic impacts.

In the present study, we explore the impact of mutations at two strigolactone biosynthesis genes, *CCD8* and *LGS1,* on sorghum physiology, growth, and biotic interactions with parasitic

plants and arbuscular mycorrhizal fungi to ask the following questions: (Q1) How does variation at strigolactone biosynthesis genes in sorghum impact biotic interactions with *Striga* and arbuscular mycorrhizae fungi? (Q2) What regulatory pathways may be altered in mutants of strigolactone biosynthesis genes and do phenotypic changes match the altered pathways? (Q3) How does variation at strigolactone biosynthesis genes in sorghum affect sorghum performance and physiology? (Q4) Are strigolactone impacts consistent across diverse genetic backgrounds?

Materials & Methods

Generation of mutants

We studied loss-of-function at the genes, *CCD8* and *LGS1*, using gene-edited *S. bicolor* of two different genetic backgrounds (Table 1). CRISPR-Cas9 edited lines of the *SbCCD8b* isoform in the 'RTx430' background were included in our study for evaluation of a strigolactone deficient line (RTx430_*ccd8b*, see greater detail in Hao et al., 2023). Sorghum genotypes have natural variation at the *LGS1* locus, impacting its functionality, and we included genetic backgrounds ('Macia' and 'RTx430') to begin to characterize how *LGS1* interacts with genetic background. Functional *LGS1* was knocked out in the normally *LGS1*-functional background 'Macia' using CRISPR-Cas9 to produce independent genome-edited lines (Macia_*lgs1*, see greater detail in Bellis et al. 2020). Unless otherwise indicated, we used a more advanced version of the material described in Bellis et al. (2020) which was backcrossed to the recurrent background 'Macia' and selfed for an additional generation (BC_0F_2) in this study (See Supplementary Methods).

The RTx430 (PI 655996) background carries the *lgs1-2* allele, which contains a large deletion that spans three predicted genes, including the sulfotransferase *LGS1* (Gobena et al.,

174 2017). Functional *LGS1* was inserted via transformation with *Agrobacterium* into the natural
175 loss-of-function background RTx430, to produce two independent mutants with restored
176 functionality of the locus (RTx430_*LGS1*) (See Supplementary Methods). For both *LGS1*
177 insertion (RTx430) and deletion events (Macia), null event mutants were also produced and
178 included in our analysis as "wild-type like" (WT-L) comparisons. Unless otherwise indicated, we
179 studied 11 genotypes in total (Macia background: Macia wild type, two *LGS1* deletion lines from
180 a normally functional background (Macia_*lgs1*), two complementary null segregants (Macia
181 WT-L); RTx430 background: RTx430 wild type, two *LGS1* insertion lines from a normally
182 non-functional background (RTx430_*LGS1*), two complementary null segregants (RTx430
183 WT-L), and a *CCD8* deletion line (RTx430_*ccd8b*).
184
185 *Striga germination assay*
186 Root exudates of the RTx430_*LGS1* insertion mutants, "wild type-like" (WT-L) null
187 segregants, and the RTx430 wild type were collected to test their *Striga* germination activity.
188 Plants were grown in a greenhouse in University Park, PA (16-hour photoperiod; day
189 temperature 28°C; night temperature 22°C). Sorghum seeds were surface sterilized in 1.2%
190 sodium hypochlorite for 10 minutes, rinsed with sterile deionized water (diH_2O) and germinated
191 in autoclaved vermiculite. One-week old seedlings were transferred to a hydroponics system
192 comprising 50 mL falcon tubes filled with half-strength modified Hoagland solution. Each
193 seedling was suspended in the solution by a bottomless 1.5 mL centrifuge tube held at the center
194 of the 50 mL falcon tube cap (J. Y. Wang et al., 2022). Plants were grown in this medium for
195 seven days and tubes were manually agitated every other day to improve airflow. The medium
196 was discarded, then tubes and seedling roots rinsed with diH_2O. Tubes were refilled with

197 half-strength Hoagland's solution without phosphate, and seedlings grown for an additional 7
198 days. Root exudates were collected in 50 mL diH_2O over a 48-hr period under darkness. Each
199 seedling's root volume was recorded by water displacement in a graduated cylinder, and exudate
200 concentrations standardized to the lowest recorded root volume prior to use for induction of
201 *Striga* germination.

202 *Striga* germination ability of root exudates was tested on parasitic seeds collected from
203 sorghum-grown fields in Kibos, Kenya and Siby, Mali (Bellis et al. 2020). Since *Striga* requires
204 conditioning to be responsive to germination stimulants (Matusova et al., 2004), *Striga* seeds
205 were surface sterilized in 1.2% sodium hypochlorite with a drop of Tween 20 for 20 mins, rinsed
206 thoroughly with sterile diH_2O, and incubated at 30°C in the dark for 10 days. After conditioning,
207 the *Striga* seed-diH_2O mixture was homogenized before pipetting 100 µL (approximately 100
208 *Striga* seeds) into a single well of a 12-well microtiter plate (CytoOne). Excess water was
209 aspirated out of the wells before adding 3 mL of sorghum root exudates. 15 biological replicates
210 of each sorghum genotype, and 2 technical reps (wells per biological rep) were tested for
211 germinability of each *Striga* population. A similar volume of 0.1ppm GR24 (synthetic
212 strigolactone standard) and diH_2O were used as positive and negative controls, respectively.
213 *Striga* germination, characterized by emergence of a radicle, was checked after incubating the
214 plates for 48 hours at 30°C in the dark, and quantified by calculating the percentage of
215 germinated *Striga* seeds in each well.
216

Identifying potential transcription factor binding sites characterizing differential gene expression in lgs1 deletion plants

Using previously generated transcriptome data from Bellis et al. 2020, we sought to identify impacted regulatory pathways in Macia_*lgs1* plants. We used samtools v1.10 (H. Li et al., 2009) to extract the 1000 bp upstream and downstream regions of the differentially expressed genes in roots and shoots separately. Specifically, we extracted the 500 bp upstream of the gene's start codon for the upstream regulatory coding region, and the 500 bp downstream of the gene's end codon for the downstream regulatory coding region. We then used STREME (Bailey, 2021) to calculate significantly enriched motifs within the differentially expressed genes in roots and shoots in contrast to non-differentially expressed genes within each specific tissue. We searched for overlaps between the discovered enriched motifs and the JASPAR 2020 CORE (Anon) plant transcription factor binding sites database (Sandelin et al., 2004) with MEME suite's online tool TOMTOM (Gupta et al., 2007).

Growth conditions for mycorrhizal assay

We tested for differences in *LGS1* and *CCD8* functional and non-functional genotypes in two genetic backgrounds under variable phosphate levels and grown with and without mycorrhizae. Plants were grown in a greenhouse in University Park, PA (16-hour photoperiod; day temperature minimum 21°C and maximum 28°C; night temperature minimum 21°C and maximum 26°C; relative humidity 20%) and subjected to three treatments: high phosphate without mycorrhizae (P+ AMF-), low phosphate without mycorrhizae (P- AMF-), and low phosphate with mycorrhizae (P- AMF+). Plants were harvested and destructive measurements were collected at two timepoints, 21 and 42 days after germination (DAG) (n = 7 per genotype,

240 treatment, and time point; total *n* = 462). The plants were grown in 10 inch "deepots" (Stuewe &
241 Sons Inc., https://stuewe.com/product/2-5-x-10-heavyweight-deepot-cell/) in a mix of 90%
242 sterile silica sand (Quickrete) and 10% kaolin clay (CB Minerals,
243 https://cbminerals.com/kaolin/). After sowing, pots were watered with tap water every day until
244 seven days after plant germination. One-week post-germination, plants were watered every other
245 day with 200 mL water and treated with a supplemental fertigation of 1/3 Hoagland with
246 different phosphate concentrations every other watering (every 4 days) until time of harvest. The
247 phosphate level of the nutrient solution used at each fertigation was 333 μM for the high
248 phosphate treatment or 33 μM for the low phosphate treatments. Pots with a mycorrhizal
249 treatment were inoculated with 50 mL of a sandy mix containing ~20 spores/mL of *Rhizophagus*
250 *intraradices* prior to planting. Spores used for inoculation were bulked in University Park, PA in
251 Spring 2023.
252 The non-destructive measurements of photosynthetic rate (steady state, measured via
253 LI-6400), chlorophyll fluorescence and stomatal conductance (measured via LI-600
254 fluorometer/porometer), and shoot traits (plant height, vegetative phase change characteristics)
255 were measured on greenhouse-grown plants prior to harvest dates. At the time of harvest (21 and
256 42 DAG) several destructive measurements were taken, and root tissue was collected for
257 quantification of mycorrhizal colonization. Above ground tissue was collected and dried in an
258 oven at 70°C for 72 hours prior to collecting dry biomass. Fresh weight of the entire root system
259 was measured. For the low phosphate non-mycorrhizal and mycorrhizal treatments, root systems
260 were divided into biopsy cassettes (Fisher Scientific) for staining to quantify mycorrhizal
261 colonization and confirmation of uncontaminated negative controls.
262

Collection of root phenotypes

Parameters of root system architecture and anatomy were collected for plants grown in the high phosphate no mycorrhizae treatment at the 42 DAG time point. To characterize architecture, entire root systems were scanned on an Epson scanner and processed in RhizoVision Explorer v2.0.3 (Seethepalli et al., 2021; Seethepalli & York, 2020) using algorithms described by (Seethepalli et al., 2021). For anatomy, we then collected two representative axial roots from node three and excised two four-cm root samples five to nine cm from the most basal portion of the whole root sample. Root samples were stored in 75% ethanol until being sectioned by laser ablation tomography (LAT; (Strock et al., 2019)). In LAT, a sample is moved via an automatic stage towards a 355-nm Avia 7000 pulsed laser and ablated in the focal plane of a camera. A Canon T3i camera with a 53micro lens (MP-E 65 mm) was used to capture images of the root cross-section. Two representative images for each root sample sectioned one to three cm apart were saved for later image analysis with Rootscan (https://plantscience.psu.edu/research/labs/roots/methods/computer/rootscan) (Burton et al., 2012). Anatomical phenotypes were averaged for each nodal root of a plant, each anatomical value was reported as the average of two roots for each node and two sections of each root.

Quantification of chlorophyll content and light harvesting proteins

We assessed if chlorophyll content (Chl*a*/Chl*b*), and concentration of photosystem proteins (ratio of *PSAA*/*CP43* and *LHCB1*/*CP43*) were altered in sorghum genotypes segregating for functional *CCD8* and *LGS1*. Plants were watered every day for the first week and then every other day until time of harvest. At every other watering, plants were supplementally fertigated with 1/3 Hoagland solution. At the time of harvest, 5-week-old plants were flash frozen in liquid

286 nitrogen. Chlorophylls were extracted from leaf tissue and thylakoid samples in acetone 80%
287 and the absorption spectra were analyzed using the Cary and fitted as previously described
288 (Croce et al., 2002).

289 Total proteins were extracted by grinding the frozen leaf tissue in a mortar with the
290 BufferA/4 from (Schägger, 2006) (3% SDS (wt/vol), 1.5% mercaptoethanol (vol/vol), 7.5%
291 glycerol (wt/vol), 0.012% CoomassieblueG-250 (Serva), 37.5mMTris/HCl (pH7.0))
292 supplemented with protease inhibitor (cOmplete™ Protease Inhibitor Cocktail (Roche)).
293 Samples were then centrifugated and the supernatant was stored at -20°C. Immunoblotting was
294 performed as described in (Schägger, 2006). All primary antibodies, PsaA(AS06172),
295 PsbC(AS111787), and LHCB1(AS01004), were purchased from Agrisera, Sweden.
296 Chemilluminescence was collected by a LAS 4000 Image Analyzer and analyzed with the
297 software ImageJ.

298

299 *Mycorrhizae counting assay*

300 To test for differences in colonization of the fungal species *R. intraradices* in sorghum
301 host plants segregating for functional *LGS1* and *CCD8*, root samples of the mycorrhizal
302 treatments stored in biopsy cassettes from both harvest time points (21 and 42 DAG) were
303 stained (https://invam.ku.edu/staining-roots) and measured for relative mycorrhizal colonization
304 (https://www2.dijon.inrae.fr/mychintec/Protocole/protoframe.html) (Koske & Gemma, 1989;
305 McGONIGLE et al., 1990; Phillips & Hayman, 1970). At the time of harvest, cassettes were
306 packed with ~0.1 grams of root system and placed in 75% EtoH until time of staining. Roots
307 were cleared using 10% KOH that was brought to boiling and then removed from the heat prior
308 to adding cassettes. Cassettes containing root samples were left in the hot KOH solution for 10

309 minutes. Samples were then washed five times using diH_2O and acidified by being immersed in a
310 2% HCl solution for 20 minutes at room temperature. After acidification, roots were stained from
311 incubation in a mixture of 1:1:1 water, glycerin, and lactic acid containing 0.05% direct blue at
312 room temperature for at least 12 hours. Stained samples were again rinsed with diH_2O five times
313 and stored suspended in diH_2O in a fridge at 15°C for one week to allow for excess leaching of
314 the stain prior to quantification of mycorrhizae.

315 Relative mycorrhizal colonization was quantified using a modified version of the grid
316 line intersect method (Giovannetti & Mosse, 1980; Newman, 1966; Tennant, 1975). Stained
317 roots were randomly dispersed in a nine-cm diameter petri plate with an acetate sheet containing
318 10x10 grid lines under the petri plate. Using an Amscope SM-2, intersections where a root
319 crossed a grid line were designated as either non-mycorrhizal or colonized. The presence of any
320 fungal structure (intracellular hyphae, vesicles, arbuscule, spore) resulted in the intersection
321 being scored as "colonized". To assess the relative abundance of mycorrhizae in each sample,
322 100 intersections were scored, and relative colonization was calculated as a percentage.

323

324 *Photosynthesis and stomatal conductance*

325 All photosynthesis measurements were measured from plants of the high phosphate
326 non-mycorrhizal treatment using a Li-6400 portable photosynthesis machine (Li-Cor
327 Environmental) after samples acclimated to the starting chamber conditions. For all
328 measurements, a constant leaf temperature of 25°C, light level of 1800 µmol m^{-2} s^{-1}, and a flow
329 rate of 400 µmol s^{-1} were maintained. Light saturated photosynthetic rate (A_{sat}) was measured at
330 a reference CO_2 level of 400 ppm. A_{sat} was recorded every 20 seconds for two minutes and
331 reported as the average across all data points logged.

332 The Li-600 Porometer/Fluorometer machine (Li-Cor Environmental) was also used to
333 measure stomatal conductance and parameters of dark (leaves were kept in the dark for a
334 minimum of 30 minutes) and light-adapted chlorophyll fluorescence. For all samples, light and
335 dark-adapted measurements were collected on the same leaves with the fixed flow rate set to
336 high (150 µmol s^{-1}) and a flash intensity of 6000 µmol m^{-2} s^{-1}.

337 We further obtained CO_2 response curves and ran untargeted metabolomics for the
338 previous generation of Macia_*lgs1* CRISPR deletion mutants using plant material as described in
339 (Bellis et al., 2020) in a separate greenhouse experiment. Plants were grown in a media mix that
340 consisted of 80% commercial sand (Quickrete) and 20% turface (LESCO turface,
341 https://www.siteone.com/en/088782-lesco-turface-all-sport-soil-conditioner-infields-50-lb/p/237
342 95) for 16-hour days. After germination, plants were watered with 100 mL of water every other
343 day and supplementally fertigated with 100 mL half strength Hoagland once a week starting at 7
344 DAG. CO_2 response curves were built by measuring net photosynthetic rate (A_{net}) at the reference
345 CO_2 levels of 50, 100, 200, 300, 400, 600, 800, 1000 ppm. Across all CO_2 levels, a constant leaf
346 temperature of 25°C, light level of 1800 µmol m^{-2} s^{-1}, and a flow rate of 400 µmol s^{-1} were
347 maintained. Leaves were given a chance to acclimate to the chamber CO_2 conditions for at least
348 two minutes before data logging at each CO_2 level. We used methods described in (Zhou et al.,
349 2019) to fit A_{net} - C_i curves and to determine apparent V_{cmax} and apparent J_{max} using procedures of
350 (Sharkey et al., 2007), accounting for carbonic anhydrase activity.

351

352 *Metabolomics*

353 To quantify differences in abundance of small molecules, root and shoot tissue samples
354 were taken for five separate plants of the following genotypes: RTx430 wild type,

355 RTx430_*ccd8b*, Macia wild type, and the earlier generation of Macia_*lgs1* deletion lines (as
356 described in Bellis et al. 2020) for untargeted metabolomics analysis. Root and shoot samples
357 were immediately flash-frozen separately in liquid nitrogen and transferred to a 1.5 mL
358 Eppendorf tube for further processing. Samples were then lyophilized at -80ºC overnight before
359 being ground to a fine powder by placing a metal ball in each Eppendorf tube and shaking in a
360 TissueLyser II (Qiagen) for 5 minutes at 25 Hz.

361 All solvents were chromatography grade and acquired from VWR (Radnor, PA, U.S.A.)
362 or Sigma Aldrich (St. Louis, MO, U.S.A.). Metabolites were extracted using 1 mL 80% MeOH +
363 0.1% formic acid for every 100 mg of powdered sample. Samples were vortexed for 10 seconds
364 and sonicated for five minutes. Then, each sample was centrifuged at 10,000 rpm for 10 minutes
365 and the supernatant was transferred to a 1 mL glass scintillation vial. The extraction process was
366 repeated with the same tissue and the supernatants were combined before being air-dried to
367 completion in a fume hood. All samples were reconstituted at a concentration of 1 mg/mL in
368 LC-MS grade methanol with 1 uM chlorpropamide as an internal standard. A Vanquish Duo
369 UHPLC system connected to a Thermo Fusion Lumos Orbitrap Mass Spectrometer (Thermo
370 Fisher Scientific, Waltham, MA) was used for metabolomics analysis with a Waters Acquity
371 UPLC BEH C18 (21.x150 mm x 1.7 um) column. The flow rate was 0.1 mL/min at 55°C.
372 Solvent A was 0.1% formic acid (v/v) in LC-MS water and solvent B was 0.1% formic acid (v/v)
373 in LC-MS acetonitrile. The mobile phase gradient of solvent B was: 3% for 0.01 minutes, 45%
374 for 10 minutes, 75% for 2 minutes, 100% for 4.5 minutes, and 3% for 0.2 minutes. A 2 ul
375 injection was used for all samples.

376 Mass spectrometry was conducted using an electrospray ionization source with a positive
377 ion spray voltage of 3500 V, sheath gas pressure of 25 Arb, auxiliary gas pressure of 5 Arb, ion

transfer temperature of 275°C, and vaporizer temperature of 75°C. MS1 data was acquired with an Orbitrap resolution of 120,000, scan range of 100-1000 Da, and RF lens of 50% in the profile mode. MS2 data was collected in a data-dependent manner using intensity (2.5E4) and dynamic exclusion (ions excluded after 1 detection for 30 seconds).

All .raw mass spectral files were converted to .mzML using MSconvert (Proteowizard) and then loaded into MzMine3.1 (Schmid et al., 2023). Root and shoot files were analyzed separately. Supplemental Table 5 outlines the MZMine3 processing parameters. Following processing in MzMine3.1, all features with a peak area less than 5-fold the intensity of the metabolite concentration in the blanks were removed. The peak area was Hellinger transformed and auto-scaled. To make volcano plots, the compounds' *P*-values and $\log_2$fold changes were calculated between each mutant and its corresponding wild type. Compounds with a $\log_2$fold change greater than 0.6 and a *P*-value less than 0.05 were labeled as "upregulated" and those with a $\log_2$fold change less than 0.6 and a *P*-value less than 0.05 were labeled as "downregulated." Key compounds were annotated by comparing their MS2 profiles to potential matches found via molecular networking performed using the Global Natural Products Social Molecular Networking (GNPS) library search feature (M. Wang et al., 2016). To compare statistical differences between mutants and their respective wild type lines, a Permutational Multivariate Analysis of Variance (PerMANOVA) was performed using the R/vegan (Oksanen et al., 2022).

Statistical analysis

To test for significance of exudate germinability of *Striga*, we built negative binomial regression models and accounted for the fixed effect of allele and the random effect of

transformation event using R/MASS::glm.nb (Venables & Ripley, 2002). For all other collected phenotypes, we tested for the significance of *LGS1* deletion and *LGS1* insertion alleles by building linear mixed effects models using R/lme4::lmer (Doran et al., 2007), again accounting for the fixed effect of allele and the random effect of transformation event. Separate models were built for plants of the Macia and RTx430 background. For *CCD8* deletions, we used a student's t-test to assess significance of the deletion allele. R statistical software (R Core Team, 2022) was used throughout for data processing and statistical analysis.

Results

Inserting functional LGS1 into a non-functional background restores Striga susceptibility

We first sought to confirm that the new (previously unpublished) mutants with functional *LGS1* inserted in a non-functional background (RTx430_*LGS1*) changed strigolactone profiles in a manner consistent with the deletion effects; i.e if *LGS1* deletions cause a shift from 5-deoxystrigol to orobanchol (Gobena et al., 2017). We tested for differences in sorghum exudate effects on germination of two *S. hermonthica* ecotypes known to be differentially sensitive to 5-deoxystrigol and orobanchol (Q1) (Bellis et al., 2020). Root exudate collected from the RTx430_*LGS1* insertion mutants resulted in significantly higher germination of both *S. hermonthica* ecotypes (Kibos, Kenya and Siby, Mali) as compared to RTx430 WT-L null segregants ($\chi^2 = 53.95$, $P < 0.001$, likelihood ratio test for fixed effect of *LGS1* deletion; Figure 1). We found the impact of functional *LGS1* in the RTx430 genetic background to be specific to the parasite ecotype, suggesting genetic variation in parasite sensitivity to host strigolactones. We observed <0.02% germination of *S. hermonthica* from Siby, Mali treated with exudate from RTx430 WT-L plants and an average germination rate of 6.5% when treated with exudate from

424 RTx430_*LGS1* plants. For the *S. hermonthica* ecotype from Kibos, Kenya, there was a
425 germination rate of <1% when treated with RTx430 WT-L exudate and an average germination
426 rate of 10.56% when treated with exudate from RTx430_*LGS1*. This result of variation in *Striga*
427 ecotype germinability is consistent with previous reports in Bellis et al. (2020), which tested
428 *LGS1* CRISPR deletions of functional alleles in the Macia background (Macia_*lgs1*).
429 Interestingly, this Kenyan *S. hermonthica* population was previously reported to have equal
430 sensitivity to 5-deoxystrigol and orobanchol (Bellis et al., 2020), suggesting that non-functional
431 *LGS1* alleles reduce the overall quantity of exuded strigolactone as compared to genotypes with
432 functional *LGS1*. Thus, insertion of functional *LGS1* into RTx430, a natural loss-of-function
433 background, increased the germination of *S. hermonthica,* likely due to increased exudation of
434 5-deoxystrigol and possibly an overall larger quantity of strigolactone in root exudate.
435
436 *Pathways involved in gene regulatory effects of LGS1 deletion*
437 Bellis et al. (2020) reported that deleting functional *LGS1* from the otherwise functional
438 Macia background resulted in significant changes in gene expression. In *LGS1* knockout plants
439 (Macia_*lgs1*), 505 differentially expressed genes (DEGs) were previously identified in roots (244
440 down-regulated and 261 up-regulated) and 2,167 DEGs were identified in shoots (917
441 down-regulated and 1,250 up-regulated). To identify regulatory pathways that may describe
442 observed differences in gene expression (Q2), we searched for sequence motifs in putative
443 promoter regions of DEGs using STREME (Bailey, 2021). Within putative promoter regions of
444 Macia_*lgs1* root DEGs, we discovered three enriched sequences that overlapped with 16 known
445 motifs, and within shoot DEGs we found six enriched sequences that overlapped with 92 known
446 motifs. We next sought to identify known transcription factor binding site (TFBS) motifs that

447 corresponded to the identified, enriched motifs from putative promoter regions of DEGs. For
448 roots, the most common discovered motif (*GACCGTCCATC*) was not significantly enriched in
449 DEGs ($P = 0.48$) but overlapped with members of six known TFBS families (Table S1). The
450 identity of these six TFBS families, some of whose members overlapped with the previously
451 mentioned motif, included ethylene-responsive element-binding factors (ERFs) and Squamosa
452 Promoter Binding Protein-Like (SPL) genes (overlap of discovered motif with TFBS sequences,
453 $P < 0.004$), which are involved in abiotic stress response and lateral root development and
454 nodulation, respectively (Fujimoto et al., 2000; Nasrollahi et al., 2022; Yu et al., 2015). SPLs are
455 known targets of strigolactone signaling and regulate many ERFs (Korek & Marzec, 2023)
456 indicating that some part of ERF and SPL signalling may be altered in Macia_*lgs1*. For shoots,
457 the most common discovered motif (*CCGGCAGCG*) was significantly enriched and found in 41
458 DEGs ($P = 0.002$, Table S2). Of the known TFBS overlapping with this discovered motif, the
459 majority belonged to the APETALA 2/ethylene-responsive element binding proteins
460 (AP2/EREBP) family (overlap of discovered motif with TFBS sequences, $P < 0.02$), which are
461 key regulators of leaf and floral development and participate in response to biotic and
462 environmental stress (Riechmann & Meyerowitz, 1998). As SPLs and AP2/ERFs regulate
463 numerous target genes, our findings suggest that *LGS1* loss-of-function may lead to broad
464 pleiotropic effects, specifically stress and growth responses may be disrupted in Macia_*lgs1*.
465

466 *Reduced CO_2 assimilation rate in strigolactone biosynthesis deletion mutants*

467 Given evidence that deletion of functional *LGS1* from a normally functional background
468 (Macia_*lgs1*) may result in broad and pleiotropic impacts, we then considered what
469 physiological differences may be attributable to differences in strigolactone profiles (Q3).

470 Supplemental addition of GR24 (a synthetic strigolactone analog) can increase photosynthetic
471 rate in multiple plant species and under varying types of environmental stress (Trasoletti et al.,
472 2022). Strigolactones have previously been reported to be positive regulators of light harvesting
473 genes in tomato (Mayzlish-Gati et al., 2010) and Bellis et al., (2020) found such genes
474 downregulated in Macia_*lgs1* mutants. Of the differentially expressed genes identified in Bellis
475 et al., (2020), Macia_*lgs1* knockout lines had a significant and systemic down-regulation of
476 genes involved in photosystem I, photosystem II, and light harvesting processes.

477 To implicate downstream, phenotypic effects of variation at *CCD8* and *LGS1*, we tested
478 mutant plants for differences in assimilation rate, chlorophyll content stomatal conductance, and
479 relative abundance of core light-harvesting proteins. For strigolactone deficient RTx430_*ccd8b*,
480 light-saturated net CO_2 assimilation rate (A_{sat}) was significantly reduced compared to the RTx430
481 wild type (t(10) = 2.36, P = 0.040, difference of genotypes by Student's *t*-test; Figure 2D),
482 indicating impaired photosynthesis in strigolactone-deficient sorghum. The reduction in the
483 strigolactone-deficient line may reflect alterations to stomatal behavior or alterations to
484 photosynthetic machinery. Under non-limiting conditions, we found chlorophyll a/b ratio
485 (Chl*a*/Chl*b*), the ratio between antenna complexes and PSII core (*LHCB1*/C*P43)* and between
486 PSI and PSII core proteins (*PSAA*/*CP43*) to be reduced for RTx430_*ccd8b* as compared to the
487 RTx430 wild type, though not significantly (Figure S1). Interestingly, we further observed
488 stomatal conductance to be increased in RTx430_*ccd8b*, though again not significantly, while
489 maintaining a reduced density of abaxial stomata (t(34) = -2.1684, P = 0.037, difference of
490 genotypes by Student's *t*-test; Figure S2). Thus it is unlikely that the reduced assimilation rate of
491 RTx430_cc*d8b* is due to stomatal limitations. Stomatal conductance was the most different in
492 *CCD8* deletion lines relative to the RTx430 WT earlier in growth (Figure S2C-D). Moreover,

strigolactone biosynthesis and signaling mutants have previously been characterized to have increased stomatal conductance in several species including, *Lotus japonicus* (J. Liu et al., 2015), tomato (Visentin et al., 2016) , and rice (Zhao et al., 2025), suggesting a conserved role of strigolactone signaling in regulating transpiration and water conservation.

For *LGS1* mutants, the rate of light-saturated photosynthesis was significantly decreased in the deletion mutant (Macia_*lgs1*), but was not significantly affected by the insertion mutant (RTx430_*LGS1*) when compared to each respective WT-L null segregant (Figure 2A,C). A_{sat} was reduced by 25% in Macia_*lgs1*. To determine if decreases in A_{sat} for Macia_*lgs1* was attributable to variation in the biochemistry of photosynthesis, we examined the maximum Rubisco carboxylation rate (V_{cmax}) and the maximum electron transport rate for ribulose-1,5-bisphosphate regeneration (J_{max}) modeled from A_{net}–C_i curves and traits modeled from dark and light-adapted fluorescence (measured traits included: Fv/Fm, maximum quantum efficiency of photosystem II (PSII); ΦPSII, quantum yield of PSII; NPQ, non-photochemical quenching; ETR, electron transport rate). We found both V_{cmax} ($\chi^2(1) = 5.00$, $P = 0.025$, likelihood ratio test for fixed effect of *LGS1* deletion; Figure S3D) and apparent J_{max} ($\chi^2(1) = 3.25$, $P = 0.07$, likelihood ratio test for fixed effect of *LGS1* deletion; Figure S3E) to be reduced in the Macia_*lgs1* lines but did not find any evidence for fluorescence traits to be significantly different. Differences in V_{cmax} and J_{max} may be consistent with Macia_*lgs1* maintaining fewer or smaller photosystems and differences in leaf N and N allocation. Again, we quantified chlorophyll content and relative protein ratios of antenna and photosystem proteins and for both backgrounds (Macia *LGS1* deletion, RTx430 *LGS1* insertion) and found no differences between insertion or deletion lines relative to each wild type and WT-L null segregants (Figure S1).

515 Though we observed reduced assimilation rate, our results indicated comparable relative
516 levels of chlorophyll a and b content and of core photosynthetic proteins between Macia_*lgs1*,
517 RTx430_*ccd8* and their respective wild types. Thus, strigolactone-related reductions in
518 assimilation rate for the tested genes in sorghum may instead reflect differences in
519 photosynthetic efficiency, potentially linked to Rubisco activity or activation state, as indicated
520 by differences in Macia_*lgs1* V_{cmax}. Further, the difference in photosynthetic rate between Macia
521 and RTx430, relative to *LGS1* functionality, suggests that background-specific modifiers may
522 influence downstream effects differently (Q4) and underscores the importance of evaluating
523 effects across multiple genetic backgrounds whenever possible.
524
525 *Mutation of strigolactone genes impacts the metabolome*
526 Previous research has reported differences in the metabolic profiles of unrelated,
527 non-isogenic sorghum genotypes that segregate for *LGS1* (Kawa et al., 2021) and some
528 metabolites, especially flavonols, are observed to have strigolactone-dependent accumulation
529 patterns in *A. thaliana* (Walton et al., 2016). We sought to identify any differences in the root and
530 shoot metabolome of our *CCD8* and *LGS1* knockout lines through untargeted metabolomics
531 using ultra-high performance liquid chromatography-MS/MS (UHPLC-MS/MS). For both
532 mutations, we found a significant change in metabolite intensity as compared to each respective
533 wild type (Figure S4), however, most of these shifts were in low-abundance compounds that we
534 were unable to identify via library matching and molecular networking (Table S3, S4) and did
535 not dramatically change the overall profile of the metabolome (PerMANOVA of root and shoot
536 untargeted metabolomic profiles, both genes, $P > 0.5$; Figure S5). An exception was a major shift
537 in the production of a disaccharide that we have tentatively identified as maltose, which was

538 increased in the roots and shoots of RTx430_*ccd8b* and had variable shifts amongst the
539 Macia_*lgs1* deletion lines as compared to each respective wild type (Figure S4).
540 For strigolactone deficient RTx430_*ccd8b*, the shoots and roots overall base peak
541 chromatogram (BPC) intensity was higher than the wild type, suggesting that deletion of *CCD8*
542 resulted in higher total metabolite production (Figure S4A, B). Evaluation of compounds with
543 lower abundance revealed that RTx430_*ccd8b* mutants had shifts in their overall metabolomic
544 profile and the majority of differentially accumulated metabolites were up-regulated in the roots
545 (Figure S6A). Of the metabolites that were upregulated in RTx430_*ccd8b* roots, we putatively
546 identified dihydroorotate which has been previously identified as upregulated in
547 drought-sensitive sorghum (Y. Li et al., 2022) and is consistent with observations of strigolactone
548 biosynthetic mutants' increased sensitivity to drought (Van Ha et al., 2014). Dihydroorotate
549 dehydrogenase (DHODH) is an enzyme involved in pyrimidine biosynthesis. In rice,
550 overexpression of the *OsDHODH1* gene increased the DHODH activity and enhanced plant
551 tolerance to salt and drought stresses (W.-Y. Liu et al., 2009). Though we did not detect
552 significant differences between the overall metabolome of Macia_*lgs1* as compared to the wild
553 type, we found differentially accumulated metabolites to be more down-regulated in the roots
554 and up-regulated in the shoots across all tested knockout lines (Figure S6C-H). For both *CCD8*
555 and *LGS1* loss-of-function mutants, alterations in low-abundance metabolite intensities
556 suggested some metabolic pathways were impacted, but the most abundant metabolites appeared
557 robust to loss-of-function at tested strigolactone biosynthesis genes.
558

Altered strigolactone profiles impact root architecture and anatomy

Strigolactones are well established to play key roles in modulating root architecture and more recently have been linked to root anatomical differences to optimize vessel element formation (Zhao et al., 2025), impacting underlying water usage strategies. Consistent with previous reports by Hoa et al., (2023), who demonstrated strigolactone deficient RTx430_*ccd8b* to have fewer root tips and overall smaller root systems, we observed RTx430_*ccd8b* plants to have overall smaller root systems ($t(14) = 4.54$, $P < 0.001$, difference of genotypes by Student's t-test; Figure S7A). Though RTx430_*ccd8b* plants had a lessened overall root network area, the root systems of RTx430_*ccd8b* had significantly more nodal roots ($t(14) = -3.17$, $P = 0.007$, difference of genotypes by Student's t-test; Figure S7B) that were smaller in diameter ($t(53) = -4.40$, $P < 0.001$, difference of genotypes by Student's t-test; Figure S7C) with altered root anatomical features. Most notably, RTx430_*ccd8b* had a significantly reduced total area of metaxylem vessels ($t(46) = -2.5632$, $P = 0.014$, difference of genotypes by Student's t-test; Figure S7D) by harboring smaller individual metaxylem vessels ($t(35) = -2.76$, $P = 0.0092$, difference of genotypes by Student's t-test; Figure S7F). We found evidence for variation at *LGS1* to impact root architecture and anatomy, though again differences were not consistent across genetic backgrounds. Macia_*lgs1* genotypes to had altered root anatomy in the form of significantly greater number of metaxylem vessel elements ($\chi^2(1) = 9.78$, $P = 0.002$, likelihood ratio test for fixed effect of *LGS1* deletion; Figure S8E) that were smaller in size ($\chi^2(1) = 4.82$, $P = 0.028$, likelihood ratio test for fixed effect of *LGS1* deletion; Figure S8F) though overall metaxylem vessel area was not significantly different (Figure S8D). Insertion of functional *LGS1* in RTx430_*LGS1* corresponded to a slight increase in the number of nodal roots ($t(43)=-2.715$, $P = 0.001$; Figure S9B), all other root anatomical traits were not significantly altered in

582 RTx430_*LGS1*. Interestingly, both genotypes with functional strigolactone genes knocked out
583 (RTx430_*ccd8b*, Macia_*lgs1*) had reduced metaxylem vessel size. Again, we did not observe
584 consistent trends in alterations to root architecture and anatomy as related to *LGS1* functionality,
585 further supporting that strigolactone effects may not be consistent across different genetic
586 backgrounds (Q4). Though considerable research has considered strigolactones' influence on
587 root system development, only recently SL signaling was identified to negatively control vessel
588 element formation in *Arabidopsis* (Zhao et al., 2025) and to our knowledge, ours is the first
589 report of strigolactone impacts on root anatomy in a monocot.
590
591 *Strigolactone mutations alter low phosphate response*
592 As strigolactones are rhizosphere signals, greatly regulated by phosphate availability, we
593 hypothesized that plants with loss-of-function at the strigolactone genes *CCD8* and *LGS1* would
594 have disrupted establishment of mycorrhizal symbiosis (Q1). To test this hypothesis, we
595 subjected all genotypes described in this study to three treatments differing in phosphate levels
596 and mycorrhizal inoculation: low phosphate and no mycorrhizae, low phosphate and
597 mycorrhizae, and high phosphate and no mycorrhizae (Figure S10). Across all genotypes, we
598 observed strong effects of the phosphate and mycorrhizal treatments. The application of
599 phosphate and mycorrhizal inoculation each independently increased plant height, shoot weight,
600 and root weight as compared to the low phosphate non-mycorrhizal treatment. Plants were the
601 tallest and largest in the high phosphate treatment. For all genotypes included in this study, we
602 observed stomatal conductance to be the lowest in the low phosphate no mycorrhizae treatment
603 as compared to both treatments with high phosphate and mycorrhizae (Figure S11E), suggesting
604 that the low phosphate no mycorrhizae treatment was indeed stressful.

605 Across all treatments, we observed RTx430_*ccd8b* mutants to be significantly shorter
606 (Figure S11A), with lower shoot (Figure S11B), and root weight (Figure S11C). Our
607 observations of the RTx430_*ccd8b* mutant grown in the treatment without nutrient limitation
608 (AMF- P+) were consistent with the phenotypic effects that are generally observed in
609 strigolactone biosynthetic mutants. RTx430_*ccd8b* displayed the classic strigolactone mutant
610 phenotype of increased shoot branching and tillering later in growth (data not shown), though
611 this phenotype was not observed in RTx430_*ccd8b* plants grown in either low phosphate
612 treatments with or without mycorrhizae, which may be attributable to a reduced growth rate
613 under stressful conditions. The distinct phenotypic differences observed in RTx430_*ccd8b*
614 mutants across high and low phosphate conditions suggest that loss-of-function at this
615 strigolactone biosynthesis gene indeed has pleiotropic effects, independent of nutrient
616 availability. Phenotypic effects were particularly pronounced under phosphate limitation,
617 suggesting that the PSR may be impaired in RTx430_*ccd8b* mutants.
618 There were no significant differences in root or shoot weight for Macia_*lgs1* grown in the
619 high phosphate treatment at the earlier time point (21 DAG) as compared to WT-L null
620 segregants grown in the same treatment. Macia_*lgs1* grown in the high phosphate treatment for
621 42 days had significantly lower dry root biomass ($\chi^2(1) = 4.18$, $P = 0.03$, likelihood ratio test for
622 fixed effect of *LGS1* deletion; Figure S12) and were shorter, though not significantly so ($P =$
623 0.23, likelihood ratio test for fixed effect of *LGS1* deletion) as compared to the WT-L null
624 segregants. This finding indicates that for plants grown without nutrient limitation, phenotypic
625 differences in root and shoot growth due to *LGS1* deletion may be subtle, only detectable at later
626 points in development, and *LGS1* deletion plants may benefit less from the application of
627 phosphate. Single-photon avalanche diode (SPAD)-based measurement of leaf chlorophyll

differed across treatments but was not significantly related to the functionality of *LGS1* for Macia plants (Figure S11D). Further, for plants of the RTx430 background, we did not find evidence for the functionality of *LGS1* to significantly impact root weight, shoot weight, SPAD, or plant height at either time point, again supporting that phenotypic effects related to *LGS1* functionality may not be consistent across genetic backgrounds of sorghum (Q4).

Strigolactone biosynthesis mutants show impaired colonization by mycorrhizae

At the first time point (21 DAG), RTx430_*ccd8b* plants had significantly delayed and overall reduced mycorrhizal colonization ($t(9) = -6.65$, $P < 0.001$, difference of genotypes by Student's t-test; Figure 3B), implicating *CCD8* in sorghum to be involved in the on-time and regular establishment of mycorrhizal partners. Furthermore, across timepoints (21 DAG, 42 DAG) RTx430_*ccd8b* root weight, shoot weight, and plant height remained significantly reduced as compared to wild type plants grown in the same treatment (Figure S10), suggesting a relatively low benefit from the addition of mycorrhizae for plants that have disrupted SL exudation. For RTx430 genotypes grown with and without mycorrhizae at 42 days, the relative increase in shoot weight was 20% lower for RTx430_*ccd8b* than all other RTx430 genotypes with functional *CCD8* included in this study ($t(8.2) = -4.53$, $P = 0.002$, difference of genotypes by Student's t-test; Figure 3D). Thus, loss of functional *CCD8* reduced AMF colonization and establishment. This impaired establishment, in turn, influenced the benefit mycorrhizal symbionts provided to RTx430_*ccd8b*. Our results are consistent with research on *CCD8* orthologs in other species (*D10*, rice), where loss-of-function at this core strigolactone biosynthesis gene impacts both the on time establishment and maintained expansion of

650 colonization for the beneficial symbionts (Kobae et al., 2018) and we further illustrated that
651 sorghum plants with functional *CCD8* deleted gained less benefit from mycorrhizal partners.
652 For plants of the Macia background at the 21 DAG time point, mycorrhizal colonization
653 was significantly reduced by 48% in Macia_*lgs1* as compared to the wild type and WT-L null
654 segregants ($\chi^2(1) = 11.38$, $P < 0.001$, likelihood ratio test for fixed effect of *LGS1* deletion;
655 Figure 3A, Figure S13A). At the later time point of 42 DAG, while mycorrhizal colonization
656 remained 15% lower for Macia_*lgs1* as compared to colonization for WT-L null segregants, the
657 difference in colonization was no longer significant ($\chi^2(1) = 2.48$, $P = 0.115$, likelihood ratio test
658 for fixed effect of *LGS1* deletion). Further supporting the disrupted early mycorrhizal
659 colonization for *Macia_lgs1*, at the earlier harvest time point (21 DAG), Macia wild type and
660 WT-L null segregants gained a greater benefit from the addition of mycorrhizae and had
661 significantly greater shoot weight ($t(38) = -2.69$, $P = 0.01$, Macia_*LGS1* difference between
662 treatments by Student's t-test), as compared to Macia_*lgs1* which did not show any difference in
663 shoot weight when grown in the mycorrhizal treatment (Figure 3C). Shoot dry weight between
664 Macia_*lgs1* and Macia lines with functional *LGS1* (Macia wild type and WT-L null segregants)
665 at the later time point (42 DAG) increased in a similar manner for plants grown with and without
666 mycorrhizae, indicating Macia genotypes differing in the functionality of *LGS1* were both able to
667 benefit from the addition of mycorrhizae given sufficient time to associate with the symbiont.
668 Together, we found evidence for the disruption of early mycorrhizal colonization for Macia_*lgs1*,
669 though given sufficient time, the relative colonization and benefit of mycorrhizae may be similar
670 for plants of the Macia background regardless of *LGS1* functionality. Additionally, given
671 findings by Akiyama et al. (2010) which indicate orobanchol as more effective than
672 5-deoxystrigol for induction of hyphal branching in the fungal species *Gigaspora marina*

673 (Akiyama et al., 2010), the impaired colonization of Macia_*lgs1* genotypes may also signify that
674 *LGS1* deletion causes lower total strigolactone exudation.

675 For plants of the RTx430 background, we did not find consistent evidence for the
676 functionality of *LGS1* to be associated with mycorrhizal colonization, though one RTx430_*LGS1*
677 line did have significantly higher colonization than its WT-L null segregant counterpart at the
678 earlier time point (21 DAG, Figure 3B). Similarly, though we did not observe any significant
679 trend in the relative benefit of mycorrhizae for RTx430 plants segregating for functional *LGS1*
680 on shoot dry weight though under the low phosphate non-mycorrhizal treatment, RTx430_*LGS1*
681 did have greater shoot weight under nutrient limitation without mycorrhizae. This may indicate
682 that restoration of functional *LGS1* into a normally non-functional background may contribute to
683 increased stress response at early points in growth, but further research is required to confirm this
684 result.

685

686 **Discussion**

687 Strigolactones are hormones known to be involved in numerous plant processes, acting
688 both as endogenous regulators of plant development and physiology and as exogenous signaling
689 compounds in root exudates that mediate interactions with soil microbes and parasitic plants. Our
690 study explored the impact of strigolactones in sorghum, a crop vital to semiarid regions with
691 often nutrient poor soils, by examining mutants of the strigolactone biosynthesis genes *CCD8*
692 and *LGS1*. Consistent with findings in other strigolactone-deficient mutants, we showed that
693 sorghum with non-functional *CCD8* exhibited altered phenotypes, physiological changes, and
694 disrupted establishment of beneficial mycorrhizal symbionts. Our results also highlight potential
695 trade-offs associated with *LGS1* loss-of-function, which often confers resistance to parasitic

696 *Striga hermonthica*. Here, we find *LGS1* effects to only be detectable in a background dependent
697 manner and deleting *LGS1* from a normally functional background (Macia) to impair
698 mycorrhizal colonization, impact early plant performance under low-phosphate conditions, and
699 reduce net carbon assimilation rate.

700 We hypothesized that strigolactone structural changes from loss-of-function at *LGS1*
701 would come at the cost of host fitness. Our results suggest genetic background and life
702 stage-specific trade-offs associated with deleting functional *LGS1* from a background with
703 normally functional *LGS1*. Though we found that reinserting functional *LGS1* into a normally
704 loss-of-function background (RTx430) restores susceptibility to *Striga* (via germination
705 stimulation), we did not find consistent evidence for trade-offs of the natural *lgs1-2* deletion
706 allele in this natural genotype. Across experiments, the only altered phenotype we observed in
707 genotypes of the RTx430 background with restored functionality of *LGS1* was an increased
708 number of nodal roots under nutrient unlimited (high phosphate) conditions. RTx430 is an
709 extensively used inbred sorghum line (Gurel et al., 2009) for both transformation and hybrid
710 production and our results suggest that other natural mutations in RTx430 may buffer potential
711 negative effects of the *LGS1* deletion.

712 We consistently found evidence for deletion mutants of both strigolactone biosynthetic
713 genes used in this study (*CCD8* and *LGS1*) to have disrupted stress response and development.
714 Strigolactones have crosstalk with multiple regulatory pathways and are involved in plant stress
715 response to drought, at least partly through crosstalk with abscisic acid (ABA) signaling.
716 Strigolactone deficient mutants have increased sensitivity to drought in some plants (Mishra et
717 al., 2016) that can be rescued through addition of exogenous strigolactones (Van Ha et al., 2014).
718 It is suggested that strigolactone mutants' hypersensitivity to drought can be attributed to an

719 increase in stomatal density and a slower induction of stomatal closure from ABA insensitivity
720 (J. Liu et al., 2015). We found support for RTx430_*ccd8b* strigolactone biosynthesis mutants to
721 have elevated stomatal conductance (though non-significantly) at earlier points in growth and
722 upregulated accumulation of dihydroorotate, a metabolite was previously reported to be more
723 abundant in sorghum drought sensitive genotypes (Y. Li et al., 2022). Our study also revealed
724 both RTX430_*ccd8b* and Macia_*lgs1*, where functional strigolactone biosynthesis genes were
725 knocked out, correspond to significant reductions in assimilation rate. In Macia_*lgs1*, reduced
726 assimilation was associated with a lower maximum rate of carboxylation (V_{cmax}), suggesting
727 limitations to Rubisco activity when functional *LGS1* is deleted. Relatedly, transcription factor
728 binding sites of the AP2/EREBP family, which are known to be involved in stress responses and
729 regulation of photosynthetic genes, were enriched in promoter regions of differentially expressed
730 genes of Macia *LGS1* knockouts. AP2/EREBPs have been suggested as ideal candidates for crop
731 improvement as their overexpression enhances tolerances to multiple abiotic and biotic stressors
732 (Xu et al., 2011). Under heat stress, overexpression of the *AtDREB1A* (AP2/EREBP subfamily
733 transcription factor) in Chrysanthemum plants resulted in significantly higher photosynthetic
734 capacity, and elevated activity of Rubisco (Hong et al., 2009), implicating this transcription
735 factor subfamily in the regulation of photosynthetic rate and suggesting a role in Rubisco
736 activation. Together, observed reductions in photosynthesis for Macia *LGS1* deletion may be
737 attributable to regulatory mechanisms as related to transcriptional difference underlying gene
738 expression, but this requires further investigation.

739 Many of the phenotypes altered in our SL biosynthesis mutants are known to be regulated
740 by the miR156-SPL pathway, suggesting it may contribute to the observed traits. In both the
741 RTX430_*ccd8b* and Macia_*lgs1* mutants, we observed reduced stomatal density, lower

742 mycorrhizal colonization and decreased photosynthetic rates; additionally RTX430_ccd8b
743 exhibited increased nodal root production (Aung et al., 2015; Lawrence et al., 2021; Poethig,
744 2013). These traits are consistent with a more "juvenile-like" developmental state associated
745 with elevated miR156 and reduced SPL expression. Previous studies have linked the
746 miR156-SPL pathway with SL biosynthesis and signaling. SPL proteins mediate SL signaling
747 through direct interaction with the signaling molecule DWARF53 (D53), which binds SPLs in
748 the absence of SLs suppressing their transcriptional activity (Barbier et al., 2023). Further, SPLs
749 promote expression of CCD and NCED genes, key enzymes in SL biosynthesis (Arango et al.,
750 2016). Supporting this connection, we found that SPL transcription factor binding sites were
751 enriched in promoter regions of differentially expressed genes of Macia LGS1 knockouts.
752 Additionally, the miR156-SPL pathway regulates miR172 expression, which targets AP2
753 transcription factors, another group of transcription factors identified in our analysis
754 (Ó'Maoiléidigh et al., 2021). We also found evidence that phosphate foraging and/or uptake may
755 be impacted in *LGS1* knockouts. Strigolactone biosynthesis and exudation is promoted under
756 nutrient limitation, especially low inorganic phosphate conditions, and affects various aspects of
757 root growth to improve phosphate foraging and increase the possibility of recruiting beneficial
758 mycorrhizae (Alder et al., 2012; Mayzlish-Gati et al., 2010; Ruyter-Spira et al., 2011; Sun et al.,
759 2014). Though strigolactone biosynthesis is thought to be suppressed when nutrients are in
760 excess, we found Macia_*lgs1* to have reduced root weight, shoot weight, and plant height when
761 grown under a high phosphate treatment but did not see differences in Macia lines segregating
762 for functional *LGS1* when grown under phosphate limitation. Thus, a potential pleiotropic impact
763 of loss-of-function at *LGS1* may include disrupted phosphate uptake or PSR.

764 Consistent with the recognized function of strigolactones in promoting associations with
765 root symbionts, *CCD8* knockout lines had notable impacts to root-microbe interactions. Previous
766 observations by Hao et al. (2023) demonstrated significant shifts in the root-associated
767 microbiome in *CCD8* knockout lines. In agreement with these findings, we also observed that the
768 same knockout lines exhibit significantly reduced mycorrhizal colonization and diminished
769 benefits from the fungi that were able to colonize the root cortex and establish symbiosis. We
770 also found evidence for a background where functional *LGS1* is deleted (Maica) to have the
771 trade-off of lower mycorrhizal colonization at early stages of growth. In addition to *LGS1*
772 deletions resulting in structural changes to strigolactones, there is evidence for *LGS1* CRISPR
773 deletions to have overall reduced exudation of strigolactone (Bellis et al. 2020). Thus, our result
774 of early-stage mycorrhizal colonization to be disrupted for Macia *LGS1* knockout could be due to
775 changes to strigolactone stereochemistry, reduced exudation of strigolactone, or a combination of
776 both impacts. As orobanchol and 5-deoxystrigol both stimulate the branching activity of
777 mycorrhizae (Akiyama et al., 2005, 2010), the impact to early mycorrhizal colonization may be
778 due to reduced overall exudation where at later time points *LGS1* deletions have had sufficient
779 time to signal the symbiont regardless of any reduction in strigolactone. For RTx430, we did not
780 find evidence of *LGS1* functionality to significantly impact mycorrhizal colonization, again
781 indicating that RTx430 which primarily exudes orobanchol (Hao et al., 2023) may have alleles at
782 other loci that offset impacts of the *lgs1-2* deletion or that the amount of strigolactone exuded
783 underlies the difference in mycorrhizal colonization for Macia *LGS1* deletions. Given that plants
784 may respond differently to different fungal species and strains (Angelard et al., 2010) and results
785 by (Gobena et al., 2017) suggest that the same sorghum genotype may have variation in

786 colonization rates between fungal species, our conclusions are limited to this *R. intraradices*
787 experiment.

788 Sorghum farmers in regions facing *Striga* pressure may benefit from cultivating varieties
789 with low germination stimulant activity (Ejeta, 2007; Hess et al., 1992). Improved varieties that
790 do not strongly induce *Striga* germination continue to show resistance to *Striga* populations and
791 current efforts to combat *Striga* include deploying *LGS1* loss-of-function alleles into farmer
792 preferred backgrounds. Consistent with Bellis et al., (2020), we find further evidence that
793 trade-offs may be coupled with deleting functional *LGS1* from normally functional backgrounds.
794 Our study highlights that the deployment of *LGS1* loss-of function alleles may be coupled with
795 trade-offs, which should be a consideration prior to the widespread cultivation of sorghum with
796 loss-of-function at *LGS1*. Nevertheless, results on RTx430 show that these trade-offs may be
797 mitigated, and we acknowledge that AMF colonization and photosynthetic trade-offs may be
798 preferable to crop loss due to *Striga.* Furthermore, our experiments may not capture dynamics of
799 field-grown sorghum. Our findings contribute to knowledge of strigolactone biology in sorghum
800 and consider the intricacies of coevolutionary dynamics where functional variation at a locus
801 achieves resistance to a parasite likely at a fitness cost.
802
803
804
805
806
807
808

Acknowledgements & Funding We thank Scott Diloreto and Sam Gruneberg for sharing their greenhouse and plant care expertise. We are grateful to Amanda Penn, Shiran Ben-Zeev, Diana Gamba, and Eric Nascari for their assistance with greenhouse data collection. We also thank the Corteva Sorghum transformation team for generation of RTx430 transgenic events, control environment team for taking care of and backcrossing plants, and the analysis team for molecular characterization of the material. RJHS is funded by the USDA National Institute of Food and Agriculture and Hatch Appropriations under Project No. PEN05039 and Accession No. 7008935, as well as by the USDA project "The Genetic Basis of Maize Response to Arbuscular Mycorrhizal Fungi" (Grant No. 2022-67013-38264). DS acknowledges support from the USDA National Institute of Food and Agriculture. JJK is supported by USDA NIFA and Hatch Appropriations under Project No. PEN04956 and Accession No. 7006496. JRL and JM acknowledge support from the Bill & Melinda Gates Foundation.

Author Contributions CMM, JRL, RHJS conceived and planned the research. CMM, MT, JM, EJA, AC, AC and MP performed the experiments and analyzed data. Plant genetic material was developed by DPS and HG. *Striga hermonthica* seed was collected by SR and BN. CMM, JRL, and EHL-P wrote the paper with input from all authors.

832 **Table 1** Description of plant material used in this study.

Background	Genotype	Description
RTx430	RTx430_*ccd8b*	*CCD8* CRISPR/Cas9-edited deletion line described in Hao et al., (2023).
	RTx430_*LGS1* RTx430 WT-L	Insertion mutants with functional *LGS1* introduced via agrobacterium random transformation, described in this study. Event null segregant.
Macia	Macia_*lgs1* Macia WT-L	A more advanced version of the *LGS1* CRISPR/Cas9-edited deletion variants described in Bellis et al., (2020). Event null segregant.

833

834

835

836

837

838

839

840

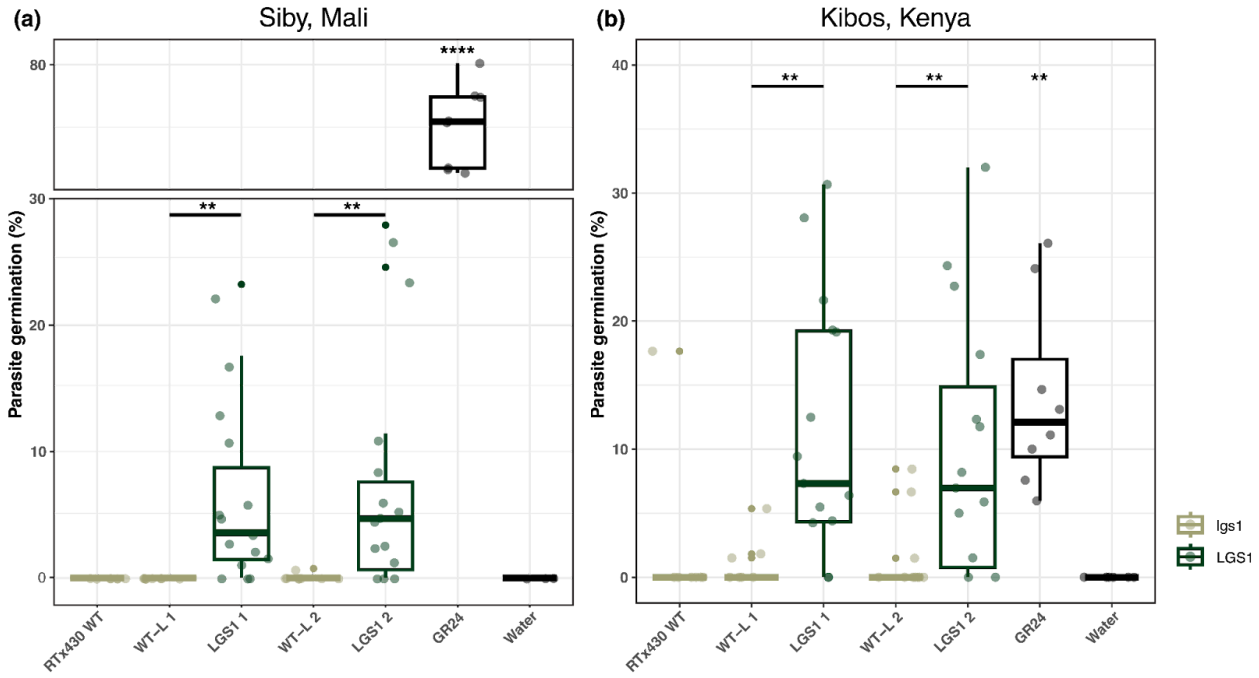

Figure 1 Restoring functional LGS1 in the RTx430 background rescues *Striga* germination. Percent *S. hermonthica* germination of two parasite populations A) Siby, Mali and B) Kibos, Kenya when exposed to root exudate from the RTx430 wild type (WT) "wild type-like" null segregants (WT-L) and LGS1 insertion mutants (LGS1), a synthetic strigolactone analog (GR24), and water. WT-L and mutants joined by a bar indicate paired genotypes that originated from the same transformation event and are denoted by 1, 2. Asterisks denote a significant P-value comparing WT-L to the mutant from the same transformation event and GR24 as compared to WT-L by t-test. **P<0.01, ****P<0.0001 (n=15). Y axis is broken for panel A.

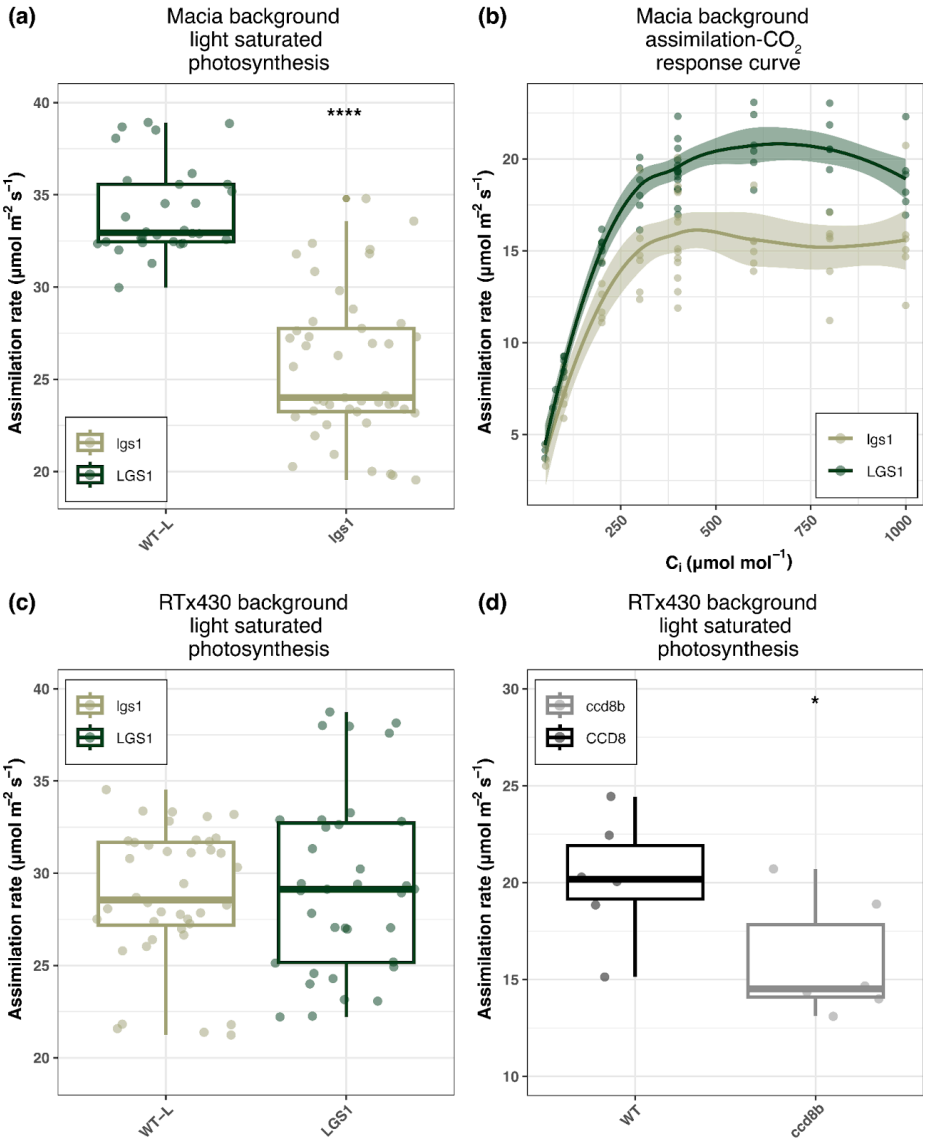

Figure 2 Light saturated assimilation rate is reduced when strigolactone biosynthesis genes are knocked out of normally functional backgrounds. A) Net carbon assimilation rate for "wild type-like" null segregants (WT-L) and *LGS1* deletion (lgs1) lines of the Macia background. B) Assimilation rate of the Macia wild type and *LGS1* deletion (*lgs1*) at varying levels of C_i. C) Net carbon assimilation rate for "wild type-like" null segregants (WT-L) and *LGS1* insertion (LGS1) lines of the RTx430 background. D) Net carbon assimilation rate for the RTx430 wild type and RTX430_*ccd8b*. Asterisks denote a significant *P*-value comparing each wild type (wild type or wild type-like) and mutant by Student's *t*-test. **P*<0.05, ****P*<0.001 (*n*=6).

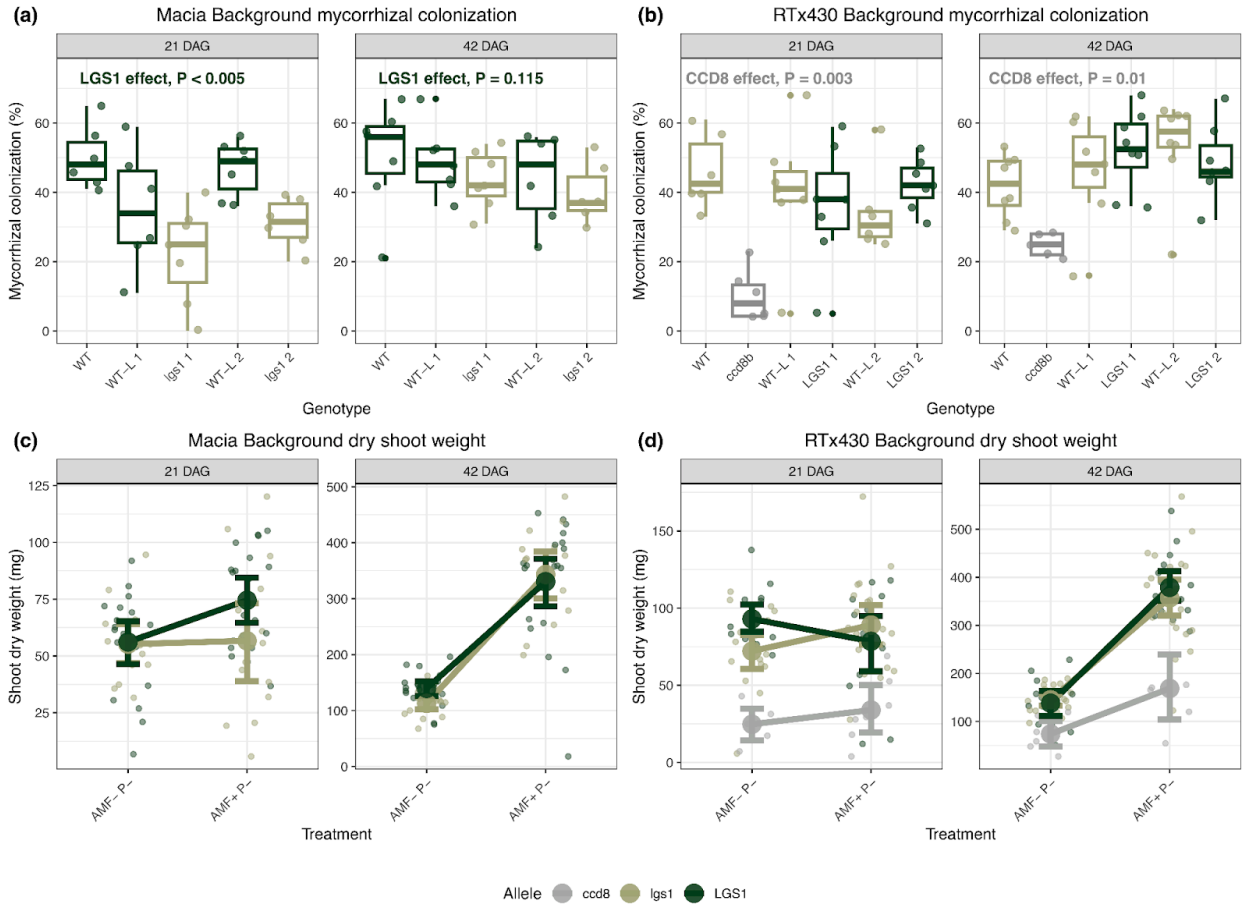

Figure 3 Mycorrhizal colonization is disrupted when strigolactone biosynthesis genes are knocked out of normally functional backgrounds. A) Percent of roots colonized by mycorrhizal species *R. intraradices* at 21 and 42 days after plant germination for wild type, "wild type-like" null segregants (WT-L), and *LGS1* deletion (lgs1) lines of the Macia background. B) Percent of roots colonized by mycorrhizal species *R. intraradices* at 21 and 42 days after germination (DAG) for wild type, *ccd8b* mutants, "wild type-like" null segregants (WT-L), and *LGS1* insertion mutants (LGS1) of the RTx430 background. WT-L and mutants denoted by 1, 2 indicate paired genotypes that originated from the same transformation event. The significance of a likelihood ratio test comparing linear mixed models that do and do not account for function at a strigolactone gene (*LGS1* or *CCD8*, respectively) as a fixed effect is reported. Dry shoot weight at 21 and 42 days after germination (DAG) for C) Macia genotypes and D) RTx430 genotypes grown under low phosphate conditions, with (AMF+ P-) and without mycorrhizae (AMF- P-). For shoot weight plots, the mean for genotypes with the same allele grown in a treatment is plotted as a dot with whiskers extending to the 95% confidence intervals.

References

Akiyama, K., Matsuzaki, K.-I., & Hayashi, H. (2005). Plant sesquiterpenes induce hyphal branching in arbuscular mycorrhizal fungi. *Nature*, *435*(7043), 824–827. https://doi.org/10.1038/nature03608

Akiyama, K., Ogasawara, S., Ito, S., & Hayashi, H. (2010). Structural requirements of strigolactones for hyphal branching in AM fungi. *Plant & Cell Physiology*, *51*(7), 1104–1117. https://doi.org/10.1093/pcp/pcq058

Alder, A., Jamil, M., Marzorati, M., Bruno, M., Vermathen, M., Bigler, P., Ghisla, S., Bouwmeester, H., Beyer, P., & Al-Babili, S. (2012). The path from β-carotene to carlactone, a strigolactone-like plant hormone. *Science (New York, N.Y.)*, *335*(6074), 1348–1351. https://doi.org/10.1126/science.1218094

Angelard, C., Colard, A., Niculita-Hirzel, H., Croll, D., & Sanders, I. R. (2010). Segregation in a mycorrhizal fungus alters rice growth and symbiosis-specific gene transcription. *Current Biology: CB*, *20*(13), 1216–1221. https://doi.org/10.1016/j.cub.2010.05.031

Arango, J., Beltrán, J., Nuñez, J., & Chavarriaga, P. (2016). Evidence of epigenetic mechanisms affecting carotenoids. *Sub-Cellular Biochemistry*, *79*, 295–307. https://doi.org/10.1007/978-3-319-39126-7_11

Arite, T., Kameoka, H., & Kyozuka, J. (2012). Strigolactone positively controls crown root elongation in rice. *Journal of Plant Growth Regulation*, *31*(2), 165–172. https://doi.org/10.1007/s00344-011-9228-6

Aung, B., Gruber, M. Y., & Hannoufa, A. (2015). The MicroRNA156 system: A tool in plant biotechnology. *Biocatalysis and Agricultural Biotechnology*, *4*(4), 432–442. https://doi.org/10.1016/j.bcab.2015.08.002

Bailey, T. L. (2021). STREME: accurate and versatile sequence motif discovery. *Bioinformatics (Oxford, England)*, *37*(18), 2834–2840. https://doi.org/10.1093/bioinformatics/btab203

Barbier, F., Fichtner, F., & Beveridge, C. (2023). The strigolactone pathway plays a crucial role in integrating metabolic and nutritional signals in plants. *Nature Plants*, *9*(8), 1191–1200. https://doi.org/10.1038/s41477-023-01453-6

Bellis, E. S., Kelly, E. A., Lorts, C. M., Gao, H., DeLeo, V. L., Rouhan, G., Budden, A., Bhaskara, G. B., Hu, Z., Muscarella, R., Timko, M. P., Nebie, B., Runo, S. M., Chilcoat, N. D., Juenger, T. E., Morris, G. P., dePamphilis, C. W., & Lasky, J. R. (2020). Genomics of sorghum local adaptation to a parasitic plant. *Proceedings of the National Academy of Sciences of the United States of America*, *117*(8), 4243–4251. https://doi.org/10.1073/pnas.1908707117

Brundrett, M. C., & Tedersoo, L. (2018). Evolutionary history of mycorrhizal symbioses and global host plant diversity. *The New Phytologist*, *220*(4), 1108–1115. https://doi.org/10.1111/nph.14976

Burton, A. L., Williams, M., Lynch, J. P., & Brown, K. M. (2012). RootScan: Software for high-throughput analysis of root anatomical traits. *Plant and Soil*, *357*(1-2), 189–203. https://doi.org/10.1007/s11104-012-1138-2

Butt, H., Jamil, M., Wang, J. Y., Al-Babili, S., & Mahfouz, M. (2018). Engineering plant architecture via CRISPR/Cas9-mediated alteration of strigolactone biosynthesis. *BMC Plant Biology*, *18*(1), 174. https://doi.org/10.1186/s12870-018-1387-1

Chien, P.-S., Chiang, C.-P., Leong, S. J., & Chiou, T.-J. (2018). Sensing and signaling of phosphate starvation: From local to long distance. *Plant & Cell Physiology*, *59*(9), 1714–1722. https://doi.org/10.1093/pcp/pcy148

Cook, C. E., Whichard, L. P., Turner, B., Wall, M. E., & Egley, G. H. (1966). Germination of witchweed (Striga lutea Lour.): Isolation and properties of a potent stimulant. *Science (New York, N.Y.)*, *154*(3753), 1189–1190. https://doi.org/10.1126/science.154.3753.1189

Croce, R., Canino, G., Ros, F., & Bassi, R. (2002). Chromophore organization in the higher-plant photosystem II antenna protein CP26. *Biochemistry*, *41*(23), 7334–7343. https://doi.org/10.1021/bi0257437

Doran, H., Bates, D., Bliese, P., & Dowling, M. (2007). Estimating the multilevel Rasch model: With thelme4Package. *Journal of Statistical Software*, *20*(2). https://doi.org/10.18637/jss.v020.i02

Ejeta, G. (2007). Breeding for *Striga* resistance in sorghum: Exploitation of an intricate host–parasite biology. *Crop Science*, *47*(S3), S – 216 – S – 227. https://doi.org/10.2135/cropsci2007.04.0011ipbs

933 Fujimoto, S. Y., Ohta, M., Usui, A., Shinshi, H., & Ohme-Takagi, M. (2000). Arabidopsis
934 ethylene-responsive element binding factors act as transcriptional activators or repressors of GCC
935 box-mediated gene expression. *The Plant Cell*, *12*(3), 393–404. https://doi.org/10.1105/tpc.12.3.393
936 Gao, J., Zhang, T., Xu, B., Jia, L., Xiao, B., Liu, H., Liu, L., Yan, H., & Xia, Q. (2018).
937 CRISPR/Cas9-mediated Mutagenesis of carotenoid cleavage dioxygenase 8 (CCD8) in tobacco
938 affects shoot and root architecture. *International Journal of Molecular Sciences*, *19*(4).
939 https://doi.org/10.3390/ijms19041062
940 Giovannetti, M., & Mosse, B. (1980). An evaluation of techniques for measuring vesicular arbuscular
941 mycorrhizal infection in roots. *The New Phytologist*, *84*(3), 489–500.
942 https://doi.org/10.1111/j.1469-8137.1980.tb04556.x
943 Giovannetti, M., Sbrana, C., Avio, L., Citernesi, A. S., & Logi, C. (1993). Differential hyphal
944 morphogenesis in arbuscular mycorrhizal fungi during pre-infection stages. *The New Phytologist*,
945 *125*(3), 587–593. https://doi.org/10.1111/j.1469-8137.1993.tb03907.x
946 Giovannetti, M., Sbrana, C., & Logi, C. (1994). Early processes involved in host recognition by
947 arbuscular mycorrhizal fungi. *The New Phytologist*, *127*(4), 703–709.
948 https://doi.org/10.1111/j.1469-8137.1994.tb02973.x
949 Gobena, D., Shimels, M., Rich, P. J., Ruyter-Spira, C., Bouwmeester, H., Kanuganti, S., Mengiste, T., &
950 Ejeta, G. (2017). Mutation in sorghum LOW GERMINATION STIMULANT 1 alters strigolactones
951 and causes Striga resistance. *Proceedings of the National Academy of Sciences of the United States*
952 *of America*, *114*(17), 4471–4476. https://doi.org/10.1073/pnas.1618965114
953 Gomez-Roldan, V., Fermas, S., Brewer, P. B., Puech-Pagès, V., Dun, E. A., Pillot, J.-P., Letisse, F.,
954 Matusova, R., Danoun, S., Portais, J.-C., Bouwmeester, H., Bécard, G., Beveridge, C. A., Rameau,
955 C., & Rochange, S. F. (2008). Strigolactone inhibition of shoot branching. *Nature*, *455*(7210),
956 189–194. https://doi.org/10.1038/nature07271
957 Gupta, S., Stamatoyannopoulos, J. A., Bailey, T. L., & Noble, W. S. (2007). Quantifying similarity
958 between motifs. *Genome Biology*, *8*(2), R24. https://doi.org/10.1186/gb-2007-8-2-r24

Gurel, S., Gurel, E., Kaur, R., Wong, J., Meng, L., Tan, H.-Q., & Lemaux, P. G. (2009). Efficient, reproducible Agrobacterium-mediated transformation of sorghum using heat treatment of immature embryos. *Plant Cell Reports*, *28*(3), 429–444. https://doi.org/10.1007/s00299-008-0655-1

Gurney, A. L., Grimanelli, D., Kanampiu, F., Hoisington, D., Scholes, J. D., & Press, M. C. (2003). Novel sources of resistance to Striga hermonthica in Tripsacum dactyloides, a wild relative of maize. *The New Phytologist*, *160*(3), 557–568. https://doi.org/10.1046/j.1469-8137.2003.00904.x

Haider, I., Yunmeng, Z., White, F., Li, C., Incitti, R., Alam, I., Gojobori, T., Ruyter-Spira, C., Al-Babili, S., & Bouwmeester, H. J. (2023). Transcriptome analysis of the phosphate starvation response sheds light on strigolactone biosynthesis in rice. *The Plant Journal: For Cell and Molecular Biology*, *114*(2), 355–370. https://doi.org/10.1111/tpj.16140

Hao, J., Yang, Y., Futrell, S., Kelly, E. A., Lorts, C. M., Nebie, B., Runo, S., Yang, J., Alvarez, S., Lasky, J. R., & Schachtman, D. P. (2023). CRISPR/Cas9-mediated Mutagenesis of *carotenoid cleavage dioxygenase* (*CCD*) genes in sorghum alters strigolactone biosynthesis and plant biotic interactions. *Phytobiomes Journal*. https://doi.org/10.1094/pbiomes-08-22-0053-r

Hess, D. E., Ejeta, G., & Butler, L. G. (1992). Selecting sorghum genotypes expressing a quantitative biosynthetic trait that confers resistance to Striga. *Phytochemistry*, *31*(2), 493–497. https://doi.org/10.1016/0031-9422(92)90023-j

Hong, B., Ma, C., Yang, Y., Wang, T., Yamaguchi-Shinozaki, K., & Gao, J. (2009). Over-expression of AtDREB1A in chrysanthemum enhances tolerance to heat stress. *Plant Molecular Biology*, *70*(3), 231–240. https://doi.org/10.1007/s11103-009-9468-z

Kawa, D., Taylor, T., Thiombiano, B., Musa, Z., Vahldick, H. E., Walmsley, A., Bucksch, A., Bouwmeester, H., & Brady, S. M. (2021). Characterization of growth and development of sorghum genotypes with differential susceptibility to Striga hermonthica. *Journal of Experimental Botany*, *72*(22), 7970–7983. https://doi.org/10.1093/jxb/erab380

Kobae, Y., Kameoka, H., Sugimura, Y., Saito, K., Ohtomo, R., Fujiwara, T., & Kyozuka, J. (2018). Strigolactone biosynthesis genes of rice are required for the punctual entry of arbuscular mycorrhizal

fungi into the roots. *Plant & Cell Physiology*, *59*(3), 544–553. https://doi.org/10.1093/pcp/pcy001

Kodama, K., Rich, M. K., Yoda, A., Shimazaki, S., Xie, X., Akiyama, K., Mizuno, Y., Komatsu, A., Luo, Y., Suzuki, H., Kameoka, H., Libourel, C., Keller, J., Sakakibara, K., Nishiyama, T., Nakagawa, T., Mashiguchi, K., Uchida, K., Yoneyama, K., … Kyozuka, J. (2022). An ancestral function of strigolactones as symbiotic rhizosphere signals. *Nature Communications*, *13*(1), 3974. https://doi.org/10.1038/s41467-022-31708-3

Kohlen, W., Charnikhova, T., Lammers, M., Pollina, T., Tóth, P., Haider, I., Pozo, M. J., de Maagd, R. A., Ruyter-Spira, C., Bouwmeester, H. J., & López-Ráez, J. A. (2012). The tomato CAROTENOID CLEAVAGE DIOXYGENASE8 (SlCCD8) regulates rhizosphere signaling, plant architecture and affects reproductive development through strigolactone biosynthesis. *The New Phytologist*, *196*(2), 535–547. https://doi.org/10.1111/j.1469-8137.2012.04265.x

Korek, M., & Marzec, M. (2023). Strigolactones and abscisic acid interactions affect plant development and response to abiotic stresses. *BMC Plant Biology*, *23*(1), 314. https://doi.org/10.1186/s12870-023-04332-6

Koske, R. E., & Gemma, J. N. (1989). A modified procedure for staining roots to detect VA mycorrhizas. *Mycological Research*, *94*, 486–488. https://doi.org/10.1016/s0953-7562(09)80692-8

Lawrence, E. H., Springer, C. J., Helliker, B. R., & Poethig, R. S. (2021). MicroRNA156-mediated changes in leaf composition lead to altered photosynthetic traits during vegetative phase change. *The New Phytologist*, *231*(3), 1008–1022. https://doi.org/10.1111/nph.17007

Li, H., Handsaker, B., Wysoker, A., Fennell, T., Ruan, J., Homer, N., Marth, G., Abecasis, G., Durbin, R., & 1000 Genome Project Data Processing Subgroup. (2009). The Sequence Alignment/Map format and SAMtools. *Bioinformatics (Oxford, England)*, *25*(16), 2078–2079. https://doi.org/10.1093/bioinformatics/btp352

Liu, J., He, H., Vitali, M., Visentin, I., Charnikhova, T., Haider, I., Schubert, A., Ruyter-Spira, C., Bouwmeester, H. J., Lovisolo, C., & Cardinale, F. (2015). Osmotic stress represses strigolactone biosynthesis in Lotus japonicus roots: exploring the interaction between strigolactones and ABA

under abiotic stress. *Planta*, *241*(6), 1435–1451. https://doi.org/10.1007/s00425-015-2266-8

Liu, W.-Y., Wang, M.-M., Huang, J., Tang, H.-J., Lan, H.-X., & Zhang, H.-S. (2009). The OsDHODH1 gene is involved in salt and drought tolerance in rice. *Journal of Integrative Plant Biology*, *51*(9), 825–833. https://doi.org/10.1111/j.1744-7909.2009.00853.x

Li, Y., Tan, B., Wang, D., Mu, Y., Li, G., Zhang, Z., Pan, Y., & Zhu, L. (2022). Proteomic analysis revealed different molecular mechanisms of response to PEG stress in drought-sensitive and drought-resistant sorghums. *International Journal of Molecular Sciences*, *23*(21), 13297. https://doi.org/10.3390/ijms232113297

Mallu, T. S., Mutinda, S., Githiri, S. M., Achieng Odeny, D., & Runo, S. (2021). New pre-attachment Striga resistant sorghum adapted to African agro-ecologies. *Pest Management Science*, *77*(6), 2894–2902. https://doi.org/10.1002/ps.6325

Maloney, G. S., DiNapoli, K. T., & Muday, G. K. (2014). The anthocyanin reduced tomato mutant demonstrates the role of flavonols in tomato lateral root and root hair development. *Plant Physiology*, *166*(2), 614–631. https://doi.org/10.1104/pp.114.240507

Matusova, R., van Mourik, T., & Bouwmeester, H. J. (2004). Changes in the sensitivity of parasitic weed seeds to germination stimulants. *Seed Science Research*, *14*(4), 335–344. https://doi.org/10.1079/ssr2004187

Mayzlish-Gati, E., LekKala, S. P., Resnick, N., Wininger, S., Bhattacharya, C., Lemcoff, J. H., Kapulnik, Y., & Koltai, H. (2010). Strigolactones are positive regulators of light-harvesting genes in tomato. *Journal of Experimental Botany*, *61*(11), 3129–3136. https://doi.org/10.1093/jxb/erq138

McGONIGLE, T. P., Miller, M. H., Evans, D. G., Fairchild, G. L., & Swan, J. A. (1990). A new method which gives an objective measure of colonization of roots by vesicular-arbuscular mycorrhizal fungi. *The New Phytologist*, *115*(3), 495–501. https://doi.org/10.1111/j.1469-8137.1990.tb00476.x

Mishra, S., Upadhyay, S., & Shukla, R. K. (2016). The role of strigolactones and their potential cross-talk under hostile ecological conditions in plants. *Frontiers in Physiology*, *7*, 691. https://doi.org/10.3389/fphys.2016.00691

Nasrollahi, V., Yuan, Z.-C., Lu, Q. S. M., McDowell, T., Kohalmi, S. E., & Hannoufa, A. (2022). Deciphering the role of SPL12 and AGL6 from a genetic module that functions in nodulation and root regeneration in Medicago sativa. *Plant Molecular Biology*, *110*(6), 511–529. https://doi.org/10.1007/s11103-022-01303-7

Newman, E. I. (1966). A method of estimating the total length of root in a sample. *The Journal of Applied Ecology*, *3*(1), 139. https://doi.org/10.2307/2401670

Oksanen, J., Simpson, G., Blanchet, F. G., Kindt, R., Legendre, P., Minchin, P., O'hara, R. B., Solymos, P., Stevens, H., Szöcs, E., & Others. (2022). vegan community ecology package version 2.6-2 April 2022. *The Comprehensive R Archive Network. Available Online: Http://cran. R-Project. Org (accessed on 15 August 2022)*. https://www.researchgate.net/publication/360782912_vegan_community_ecology_package_version_26-2_April_2022

Ó'Maoiléidigh, D. S., van Driel, A. D., Singh, A., Sang, Q., Le Bec, N., Vincent, C., de Olalla, E. B. G., Vayssières, A., Romera Branchat, M., Severing, E., Martinez Gallegos, R., & Coupland, G. (2021). Systematic analyses of the MIR172 family members of Arabidopsis define their distinct roles in regulation of APETALA2 during floral transition. *PLoS Biology*, *19*(2), e3001043. https://doi.org/10.1371/journal.pbio.3001043

Phillips, J. M., & Hayman, D. S. (1970). Improved procedures for clearing roots and staining parasitic and vesicular-arbuscular mycorrhizal fungi for rapid assessment of infection. *Transactions of the British Mycological Society*, *55*(1), 158–IN18. https://doi.org/10.1016/s0007-1536(70)80110-3

Poethig, R. S. (2013). Vegetative phase change and shoot maturation in plants. *Current Topics in Developmental Biology*, *105*, 125–152. https://doi.org/10.1016/B978-0-12-396968-2.00005-1

Rasmussen, A., Mason, M. G., De Cuyper, C., Brewer, P. B., Herold, S., Agusti, J., Geelen, D., Greb, T., Goormachtig, S., Beeckman, T., & Beveridge, C. A. (2012). Strigolactones suppress adventitious rooting in Arabidopsis and pea. *Plant Physiology*, *158*(4), 1976–1987. https://doi.org/10.1104/pp.111.187104

R Core Team. (2022). *R: A Language and Environment for Statistical Computing. R Foundation for Statistical Computing, Vienna.* https://www.R-project.org.

Riechmann, J. L., & Meyerowitz, E. M. (1998). The AP2/EREBP family of plant transcription factors. *Biological Chemistry*, *379*(6), 633–646. https://doi.org/10.1515/bchm.1998.379.6.633

Ruyter-Spira, C., Kohlen, W., Charnikhova, T., van Zeijl, A., van Bezouwen, L., de Ruijter, N., Cardoso, C., Lopez-Raez, J. A., Matusova, R., Bours, R., Verstappen, F., & Bouwmeester, H. (2011). Physiological effects of the synthetic strigolactone analog GR24 on root system architecture in Arabidopsis: another belowground role for strigolactones? *Plant Physiology*, *155*(2), 721–734. https://doi.org/10.1104/pp.110.166645

Saeed, W., Naseem, S., & Ali, Z. (2017). Strigolactones biosynthesis and their role in abiotic stress resilience in plants: A critical review. *Frontiers in Plant Science*, *8*, 1487. https://doi.org/10.3389/fpls.2017.01487

Sandelin, A., Alkema, W., Engström, P., Wasserman, W. W., & Lenhard, B. (2004). JASPAR: an open-access database for eukaryotic transcription factor binding profiles. *Nucleic Acids Research*, *32*(Database issue), D91–D94. https://doi.org/10.1093/nar/gkh012

Schägger, H. (2006). Tricine-SDS-PAGE. *Nature Protocols*, *1*(1), 16–22. https://doi.org/10.1038/nprot.2006.4

Schmid, R., Heuckeroth, S., Korf, A., Smirnov, A., Myers, O., Dyrlund, T. S., Bushuiev, R., Murray, K. J., Hoffmann, N., Lu, M., Sarvepalli, A., Zhang, Z., Fleischauer, M., Dührkop, K., Wesner, M., Hoogstra, S. J., Rudt, E., Mokshyna, O., Brungs, C., … Pluskal, T. (2023). Integrative analysis of multimodal mass spectrometry data in MZmine 3. *Nature Biotechnology*, *41*(4), 447–449. https://doi.org/10.1038/s41587-023-01690-2

Seethepalli, A., Dhakal, K., Griffiths, M., Guo, H., Freschet, G. T., & York, L. M. (2021). RhizoVision Explorer: open-source software for root image analysis and measurement standardization. *AoB Plants*, *13*(6), lab056. https://doi.org/10.1093/aobpla/plab056

Seethepalli, A., & York, L. M. (2020). *RhizoVision Explorer - Interactive software for generalized root*

image analysis designed for everyone. Zenodo. https://doi.org/10.5281/ZENODO.4095629

Seto, Y., Sado, A., Asami, K., Hanada, A., Umehara, M., Akiyama, K., & Yamaguchi, S. (2014). Carlactone is an endogenous biosynthetic precursor for strigolactones. *Proceedings of the National Academy of Sciences of the United States of America*, *111*(4), 1640–1645. https://doi.org/10.1073/pnas.1314805111

Sharkey, T. D., Bernacchi, C. J., Farquhar, G. D., & Singsaas, E. L. (2007). Fitting photosynthetic carbon dioxide response curves for C(3) leaves. *Plant, Cell & Environment*, *30*(9), 1035–1040. https://doi.org/10.1111/j.1365-3040.2007.01710.x

Sorefan, K., Booker, J., Haurogné, K., Goussot, M., Bainbridge, K., Foo, E., Chatfield, S., Ward, S., Beveridge, C., Rameau, C., & Leyser, O. (2003). MAX4 and RMS1 are orthologous dioxygenase-like genes that regulate shoot branching in Arabidopsis and pea. *Genes & Development*, *17*(12), 1469–1474. https://doi.org/10.1101/gad.256603

Spallek, T., Mutuku, M., & Shirasu, K. (2013). The genus Striga: a witch profile. *Molecular Plant Pathology*, *14*(9), 861–869. https://doi.org/10.1111/mpp.12058

Strock, C. F., Schneider, H. M., Galindo-Castañeda, T., Hall, B. T., Van Gansbeke, B., Mather, D. E., Roth, M. G., Chilvers, M. I., Guo, X., Brown, K., & Lynch, J. P. (2019). Laser ablation tomography for visualization of root colonization by edaphic organisms. *Journal of Experimental Botany*, *70*(19), 5327–5342. https://doi.org/10.1093/jxb/erz271

Sun, H., Tao, J., Liu, S., Huang, S., Chen, S., Xie, X., Yoneyama, K., Zhang, Y., & Xu, G. (2014). Strigolactones are involved in phosphate- and nitrate-deficiency-induced root development and auxin transport in rice. *Journal of Experimental Botany*, *65*(22), 6735–6746. https://doi.org/10.1093/jxb/eru029

Tennant, D. (1975). A test of a modified line intersect method of estimating root length. *The Journal of Ecology*, *63*(3), 995. https://doi.org/10.2307/2258617

Trasoletti, M., Visentin, I., Campo, E., Schubert, A., & Cardinale, F. (2022). Strigolactones as a hormonal hub for the acclimation and priming to environmental stress in plants. *Plant, Cell & Environment*,

45(12), 3611–3630. https://doi.org/10.1111/pce.14461

Urquhart, S., Foo, E., & Reid, J. B. (2015). The role of strigolactones in photomorphogenesis of pea is limited to adventitious rooting. *Physiologia Plantarum*, *153*(3), 392–402. https://doi.org/10.1111/ppl.12246

Van Ha, C., Leyva-González, M. A., Osakabe, Y., Tran, U. T., Nishiyama, R., Watanabe, Y., Tanaka, M., Seki, M., Yamaguchi, S., Van Dong, N., Yamaguchi-Shinozaki, K., Shinozaki, K., Herrera-Estrella, L., & Tran, L.-S. P. (2014). Positive regulatory role of strigolactone in plant responses to drought and salt stress. *Proceedings of the National Academy of Sciences of the United States of America*, *111*(2), 851–856. https://doi.org/10.1073/pnas.1322135111

Venables, W. N., & Ripley, B. D. (2002). *Modern applied statistics with S*. Springer. https://doi.org/10.1007/978-0-387-21706-2

Visentin, I., Vitali, M., Ferrero, M., Zhang, Y., Ruyter-Spira, C., Novák, O., Strnad, M., Lovisolo, C., Schubert, A., & Cardinale, F. (2016). Low levels of strigolactones in roots as a component of the systemic signal of drought stress in tomato. *The New Phytologist*, *212*(4), 954–963. https://doi.org/10.1111/nph.14190

Vogel, J. T., Walter, M. H., Giavalisco, P., Lytovchenko, A., Kohlen, W., Charnikhova, T., Simkin, A. J., Goulet, C., Strack, D., Bouwmeester, H. J., Fernie, A. R., & Klee, H. J. (2010). SlCCD7 controls strigolactone biosynthesis, shoot branching and mycorrhiza-induced apocarotenoid formation in tomato. *The Plant Journal: For Cell and Molecular Biology*, *61*(2), 300–311. https://doi.org/10.1111/j.1365-313X.2009.04056.x

Walton, A., Stes, E., Goeminne, G., Braem, L., Vuylsteke, M., Matthys, C., De Cuyper, C., Staes, A., Vandenbussche, J., Boyer, F.-D., Vanholme, R., Fromentin, J., Boerjan, W., Gevaert, K., & Goormachtig, S. (2016). The response of the root proteome to the synthetic strigolactone GR24 in Arabidopsis. *Molecular & Cellular Proteomics: MCP*, *15*(8), 2744–2755. https://doi.org/10.1074/mcp.M115.050062

Wang, J. Y., Chen, G.-T. E., Jamil, M., Braguy, J., Sioud, S., Liew, K. X., Balakrishna, A., & Al-Babili, S.

(2022). Protocol for characterizing strigolactones released by plant roots. *STAR Protocols*, *3*(2), 101352. https://doi.org/10.1016/j.xpro.2022.101352

Wang, M., Carver, J. J., Phelan, V. V., Sanchez, L. M., Garg, N., Peng, Y., Nguyen, D. D., Watrous, J., Kapono, C. A., Luzzatto-Knaan, T., Porto, C., Bouslimani, A., Melnik, A. V., Meehan, M. J., Liu, W.-T., Crüsemann, M., Boudreau, P. D., Esquenazi, E., Sandoval-Calderón, M., … Bandeira, N. (2016). Sharing and community curation of mass spectrometry data with Global Natural Products Social Molecular Networking. *Nature Biotechnology*, *34*(8), 828–837. https://doi.org/10.1038/nbt.3597

Wang, Y., Duran, H. G. S., van Haarst, J. C., Schijlen, E. G. W. M., Ruyter-Spira, C., Medema, M. H., Dong, L., & Bouwmeester, H. J. (2021). The role of strigolactones in P deficiency induced transcriptional changes in tomato roots. *BMC Plant Biology*, *21*(1), 349. https://doi.org/10.1186/s12870-021-03124-0

Wu, F., Gao, Y., Yang, W., Sui, N., & Zhu, J. (2022). Biological functions of strigolactones and their crosstalk with other phytohormones. *Frontiers in Plant Science*, *13*, 821563. https://doi.org/10.3389/fpls.2022.821563

Wu, S., & Li, Y. (2021). A unique sulfotransferase-involving strigolactone biosynthetic route in sorghum. *Frontiers in Plant Science*, *12*, 793459. https://doi.org/10.3389/fpls.2021.793459

Xu, Z.-S., Chen, M., Li, L.-C., & Ma, Y.-Z. (2011). Functions and application of the AP2/ERF transcription factor family in crop improvement. *Journal of Integrative Plant Biology*, *53*(7), 570–585. https://doi.org/10.1111/j.1744-7909.2011.01062.x

Yoda, A., Mori, N., Akiyama, K., Kikuchi, M., Xie, X., Miura, K., Yoneyama, K., Sato-Izawa, K., Yamaguchi, S., Yoneyama, K., Nelson, D. C., & Nomura, T. (2021). Strigolactone biosynthesis catalyzed by cytochrome P450 and sulfotransferase in sorghum. *The New Phytologist*, *232*(5), 1999–2010. https://doi.org/10.1111/nph.17737

Yoneyama, K., Awad, A. A., Xie, X., Yoneyama, K., & Takeuchi, Y. (2010). Strigolactones as germination stimulants for root parasitic plants. *Plant & Cell Physiology*, *51*(7), 1095–1103.

https://doi.org/10.1093/pcp/pcq055

Yoneyama, K., & Brewer, P. B. (2021). Strigolactones, how are they synthesized to regulate plant growth and development? *Current Opinion in Plant Biology*, *63*(102072), 102072. https://doi.org/10.1016/j.pbi.2021.102072

Yu, N., Niu, Q.-W., Ng, K.-H., & Chua, N.-H. (2015). The role of miR156/SPLs modules in Arabidopsis lateral root development. *The Plant Journal: For Cell and Molecular Biology*, *83*(4), 673–685. https://doi.org/10.1111/tpj.12919

Zhang, Z., Liao, H., & Lucas, W. J. (2014). Molecular mechanisms underlying phosphate sensing, signaling, and adaptation in plants. *Journal of Integrative Plant Biology*, *56*(3), 192–220. https://doi.org/10.1111/jipb.12163

Zhao, J., Shi, D., Kaeufer, K., Song, C., Both, D., Thier, A. L., Cao, H., Lassen, L., Xu, X., Hamamura, Y., Luzzietti, L., Bennett, T., Kaufmann, K., & Greb, T. (2025). Strigolactones optimise plant water usage by modulating vessel formation. *Nature Communications*, *16*(1), 3854. https://doi.org/10.1038/s41467-025-59072-y

Zhou, H., Akçay, E., & Helliker, B. R. (2019). Estimating C4 photosynthesis parameters by fitting intensive A/Ci curves. *Photosynthesis Research*, *141*(2), 181–194. https://doi.org/10.1007/s11120-019-00619-8